UNIVERSITY OF GHANA

SITE-SPECIFIC SOIL CLASSIFICATION OF SEISMIC SITE EFFECTS FOR THE GREATER ACCRA METROPOLITAN AREA OF GHANA USING MULTICHANNEL ANALYSIS OF SURFACE WAVES

PRESENTED

By

GRACE NORTEY

(10025634)

THIS THESIS SUBMITTED IS SUBMITTED TO THE UNIVERSITY OF GHANA, LEGON IN PARTIAL FULFILMENT OF THE REQUIREMENT FOR THE AWARD OF PHD IN EARTH SCIENCE

DECEMBER, 2021

DECLARATION

This is to certify that this is the result of research carried out by Grace Nortey towards the award of Doctor of Philosophy in Earth Science from the Department of Earth Science, University of Ghana, under the supervision of Dr. T. K. Armah and Dr. P. E. Amponsah.

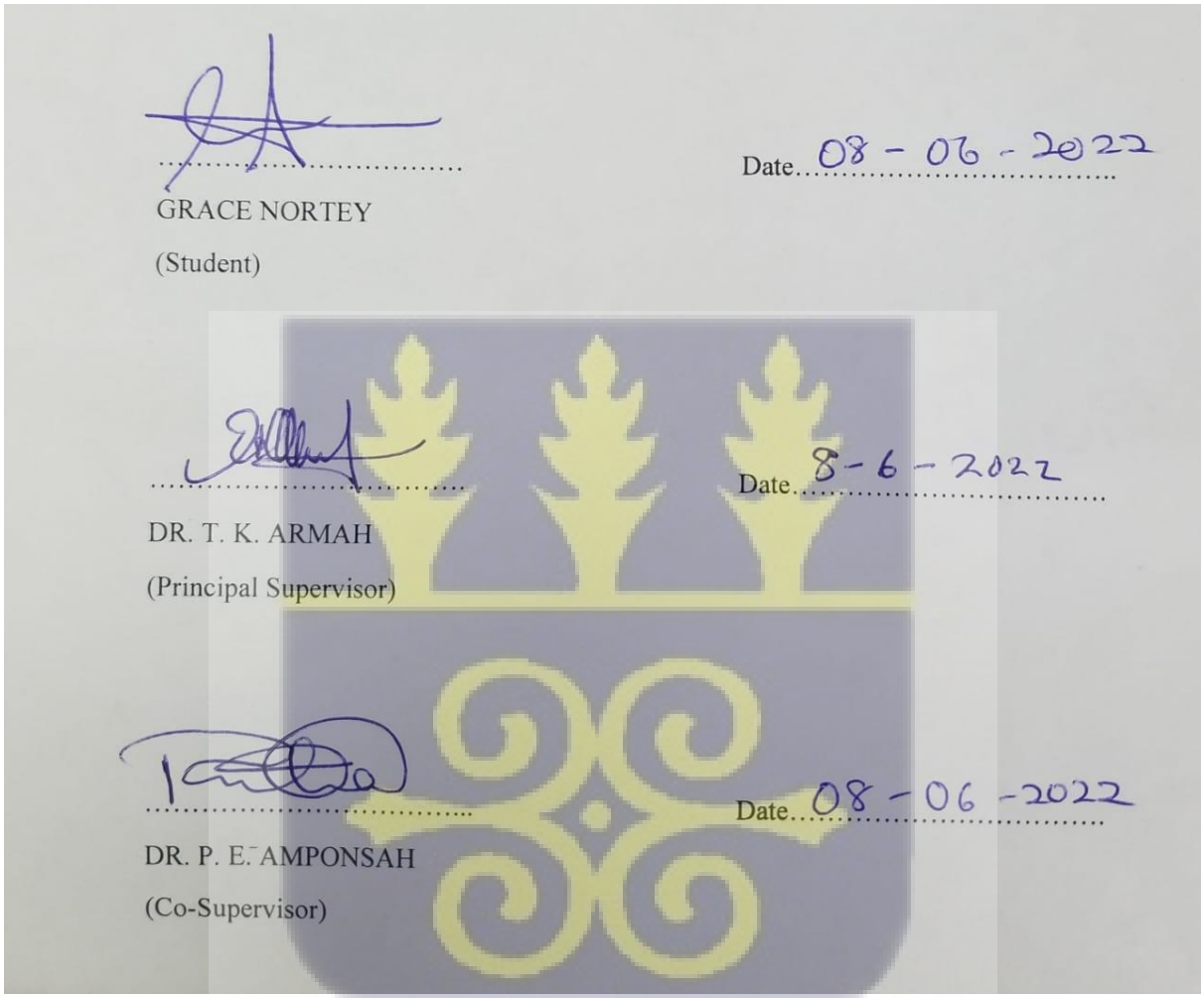

.....
GRACE NORTEY
(Student)

Date 08 - 06 - 2022

.....
DR. T. K. ARMAH
(Principal Supervisor)

Date 8 - 6 - 2022

.....
DR. P. E. AMPONSAH
(Co-Supervisor)

Date 08 - 06 - 2022

ABSTRACT

The study presents site classification for Greater Accra Metropolitan Area (GAMA) of Ghana. Multichannel analysis of surface waves (MASW) is used to calculate shear wave velocity to various depths within the study area. Calculated shear wave velocity up to a depth of 30 m has been used to assess seismic site effects and soil conditions for a major part of the GAMA. Seismic risk has become overwhelmingly apparent from many studies carried out over this area. The area is overpopulated, poorly planned, with the largest convergence of major and minor faults, as well as several historical and recent events. Despite the exposed seismic risk, a regional soils conditions map is yet to be completed for the GAMA.

Dispersion data from 42 test sites was inverted and classified according to suggested seismic site classification scheme by National Earthquake Hazard Risk Program (NEHRP).

From results of calculated shear wave velocity up to 30 m of soil, two main site classes have become apparent (D and C). Considering the geology of the underlying subsoils, two subdivisions for site class D is suggested (D1 and D2).

The residual soils to the southwest and northwest of the study area are derived predominantly from granitoids, and their response is characteristically low. These values are generally within a range of 180 -360 m/s and thus fall into suggested site class D1, the most vulnerable within the test site.

Similar to site class D1, D2 is also characterized by low shear wave velocity values (180 -360 m/s), however the underlying subsoils derived from phyllites within the study area. D2 occupies area to the southeast, lower and upper middle of the study area. Several vulnerabilities were identified for soils of site class D within the study area.

Site class C is identified mostly within the central part of the study area. Residual soils for site class C are mainly derived from the quartz-schist and quartzite units of the GAMA. They are characterized by moderate shear wave velocity response (360 -760 m/s), a transition between stiff soils to hard rock.

From calculated shear wave velocities for 5 m, 15 m, 30 m and 40 m, shear wave velocity (SWV) increases with depth for the study area. However, the SWV from 5 m up to approximately 15 m depth is characteristically low (between 180 – 360 m/s), with several dynamic features that point to many vulnerabilities in soil competency within the first 15 m for the entire region.

DEDICATION

This work is dedicated to His Excellency The Holy Spirit

My Mighty Counsellor

ACKNOWLEDGEMENTS

My heartfelt thanks go to Dr. Thomas Armah and Dr. Paulina Amponsah. Special thanks to Dr. Armah for your patience, guidance, support, and selfless devotion in always assisting me.

I am particularly grateful to Dr. K. Boamah and Mr. Nicholas Opoku of the Geological Survey Department of Ghana for facilitating data collection. My genuine gratitude to Fred Abankwah for his availability in collecting field data.

Special thanks to Mr. Michael Cantey.

TABLE OF CONTENTS

LIST OF FIGURES

LIST OF TABLES

LIST OF ABBREVIATIONS

ρ	Density
SWV	Shear Wave Velocity
k	Bulk Modulus
μ	Shear Modulus
σ	Poisson's Ratio
t	Time
x	Distance
z	Depth
f	Frequency
λ	Wavelength
λmax	Maximum Wavelength
Zmax	Maximum Depth of Penetration
C	Rayleigh-Wave Phase Velocity
p	Slowness
RMS (E)	Root Mean Square (Error)
D	Spread Length
x_1	Near Offset
PSHA	Probabilistic Seismic Hazard Analysis
MASW	Multichannel Analysis of Surface Waves
NEHRP	National Earthquake Hazards Reduction Program
IBC	International Building Code
Vs	Shear Wave Velocity
Vs30	Time for shear wave to travel from a depth of 30 m to the ground surface

IDW	Inverse Distance Weighting

CHAPTER ONE

INTRODUCTION

1.1 Background

Frequent tremors (ML 3.8 - 4.8); 1997, 2003, 20l8, 2011, 2012, 2020, following nearly a century of quiescence since a damaging earthquake (ML ≥ 6.5), has led government and relevant stakeholders to urgently push for proactive counter measures, (seismic alerts and improved Probabilistic Seismic Hazard Assessment) that will influence effective seismic design in existing and new infrastructure throughout the Greater Accra Metropolitan Area (GAMA). These measures will guide effective policy, management and contingency planning for reducing the potential catastrophic effects of a large earthquake in Ghana.

Ghana is located on the SE margin of the West African Craton (WAC), though significantly far removed from any of the present-day active tectonic plate boundaries, Ghana, and a significant portion of the Greater Accra Metropolitan area (GAMA) is seismically active (Figure 1.1) and has suffered the effects of damaging earthquakes; 1636, 1862, 1906, 1939 (Table 1.1).

Remarkable strides in development over the last 20 years or so, *(https://www.weforum.org/agenda/2019/05/ghana-is-set-to-be-the-worlds-fastest-growing economy-this-year-according-to-the-imf, accessed 01/05/2021, 17:00GMT)*, has translated into a dangerously overpopulated environment dominated by many high-rise buildings. Consequently, large areas within the GAMA, remain poorly planned, with many buildings sited on or near fracture zones (McCallien, 1962) or soft sediments (valleys, estuaries, recent deposits, unconsolidated materials etc.).

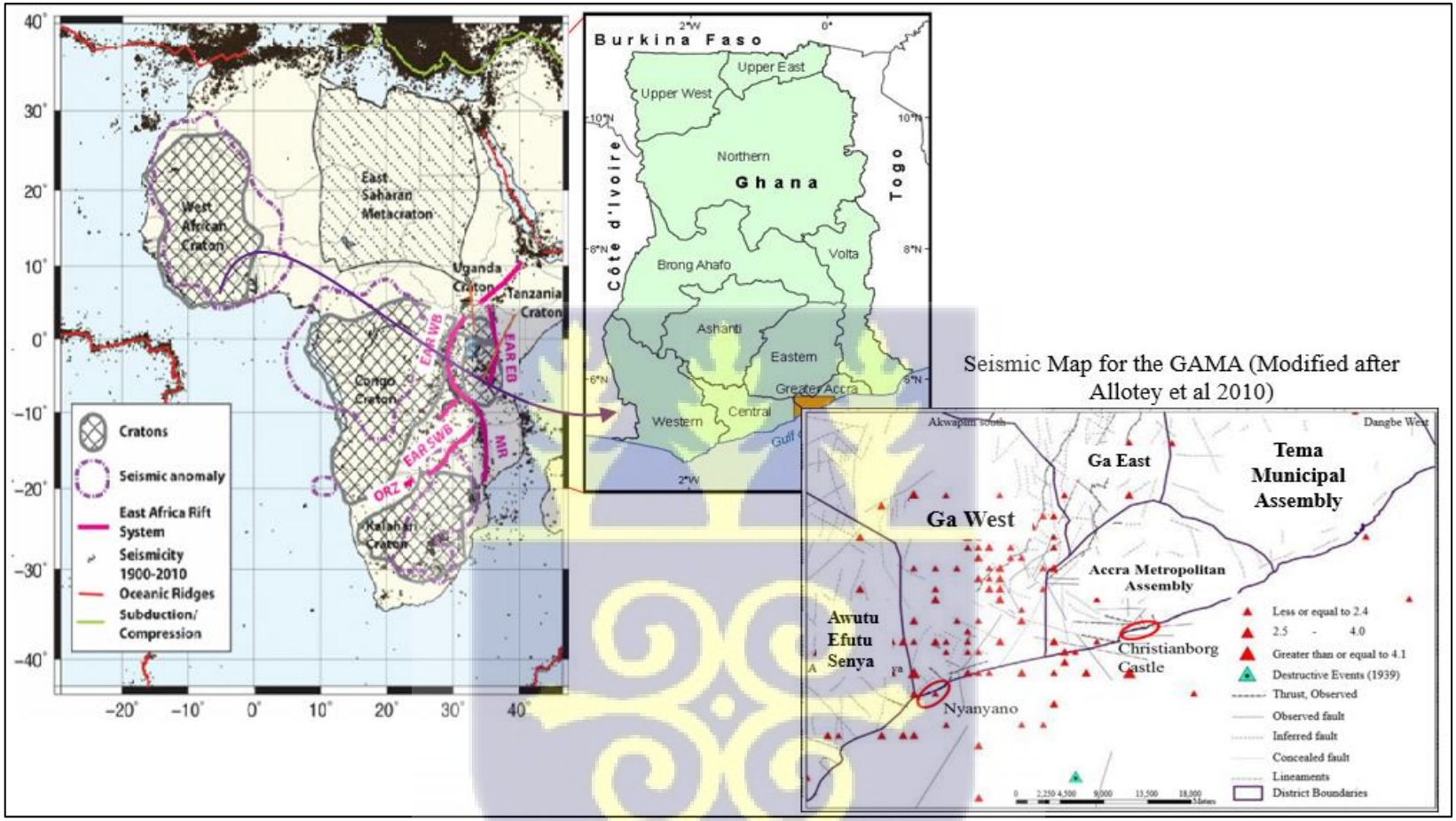

Figure 1.1 Seismic hazard map of Africa showing the relative location of the GAMA area to the major seismic regions of Africa. Insert seismic map of the GAMA (after Allotey et al., 2010)

Table 1 Ghana's Seismicity (after Amponsah et al., 2012)

Year	Magnitude	Intensity	Comments
18/12/1636	5.7	IX	Very severe. Most affected was the Axim district in the Western region of Ghana where a goldmine collapsed.
10/07/1862	6.5	IX	Very strong earthquake, severe damage in Accra and along the coast of Ghana to the Republic of Togo, most stone buildings were razed to the ground and the castle in Accra was rendered uninhabitable.
11/05/1911			Wharf at Lome was destroyed by a tsunami which was caused by an offshore earthquake
1/09/1923			A series of strong earthquake shocks lasting for over 8 hours recorded by a seismograph in Accra; details are unknown
22/06/1939	6.5	IX (estimated by Junner 1941) VIII (recalculated by Amponsah et al, 2012)	Most destructive earthquake observed in Ghana in the last century, it affected the entire county, 17 people were killed and hundreds were injured. The epicentre was offshore.
11/03/1964	4.5*	VI	A severe shock was felt in Amasaman
9/02/1969	4.7*	VI	Strong tremor was felt in Accra
1997	3.8		Felt mainly in Accra
2003	4.8		Felt in some parts of Accra
2011	4		Near Coast of Ghana Togo
2012	4.2		Near the Coast of Accra.

*Local magnitude

Several lapses in the built environment such as the regular use of different building codes (BRRI, 1990 or IBC, 2000 or 2006), for various infrastructure (EERI Housner Report 2015), and the poor construction practice of weak column strong beam, amongst others, highlight compromises in the current built environment of the GAMA, that falls below expected standard seismic criteria. These compromises continually increase the vulnerability of the metropolis to earthquakes and its affiliated disasters on a daily basis.

Since the empirical seismic measurements and damage data obtained for the development of generic overseas codes (BRRI, 1990 or IBC, 2000 or 2006), are obtained from deep soils with rather simple geology in the United States, they may not necessarily reflect regional and geotechnical soil characteristics for certain countries and may lead to variations in seismic response characteristics and underestimation of actual ground motion (Kim et al 2002, Lee et al 2012, Wills et al. 2000; Wald and Allen 2007). Consequent underestimation of soil stiffness results in severe damage to structures within the metropolis.

Soil distribution over the GAMA is complex (Figure 1.2), comprising heavy silty sandy-clays or fine to coarse sands, at lower elevations and varied lateritic type soils on higher ground (Ayetey and Andoh, 1988). Low-lying coastal areas such as Accra, Nyanyano, Sakumono, Korle Gonno, Aplaku, Tetegu, and Weija, are predominantly characterized by unconsolidated sand and clay deposits.

Seismic waves are significantly amplified on soft soils, triggering major liquefaction, due to seismic site effects (Richardt et al., 1970).

Previous broad area zonation maps have categorized these areas as most prone to major liquefaction during an earthquake (Figure 1.3). To put all this into perspective, the 1995 earthquake in Dinar Turkey (MS 6.1), killed 90 people destroyed over 4000 buildings.

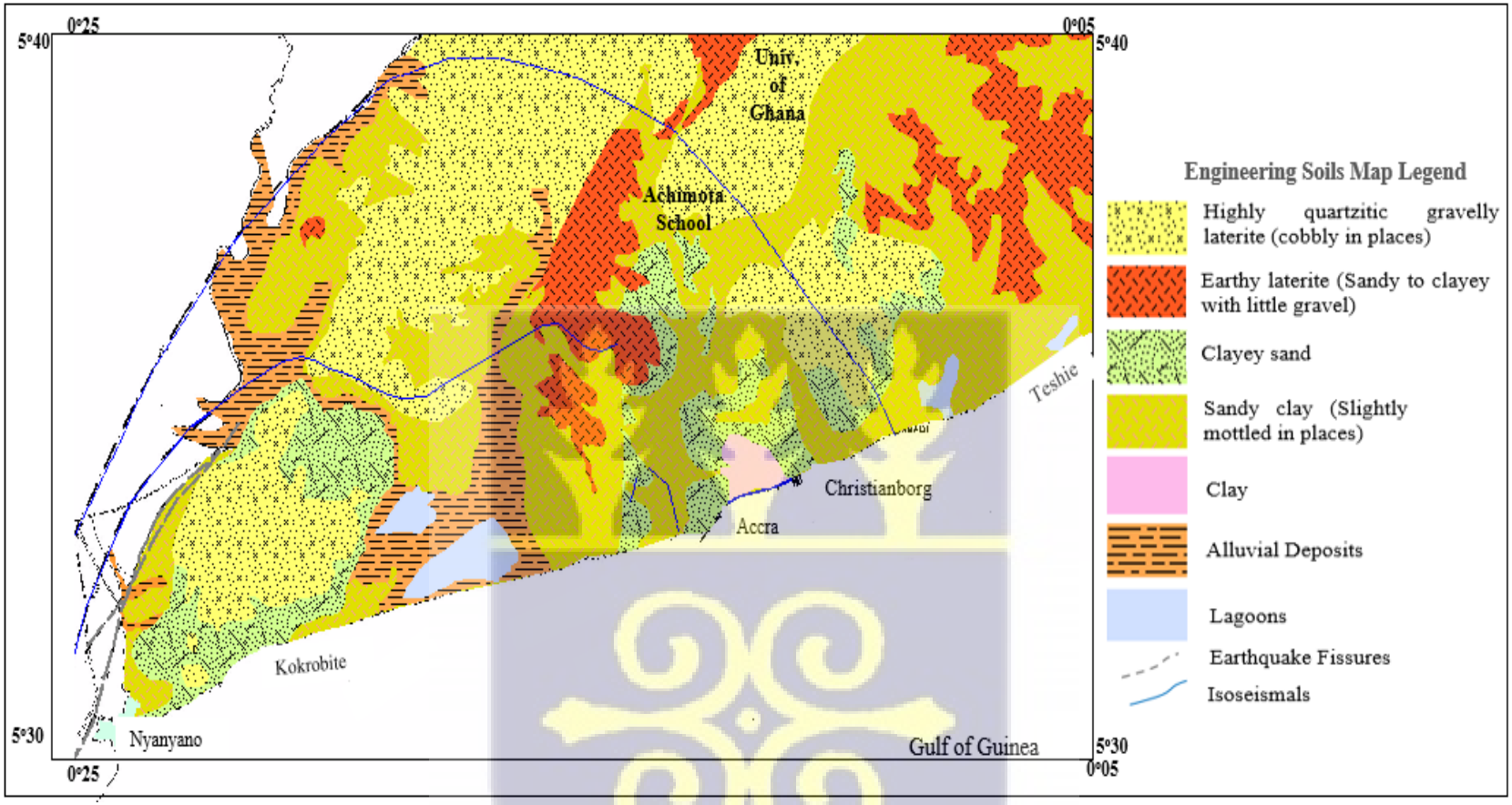

Figure 1.2 Engineering soils map and earthquake risk potential zones in Accra area showing isosiesmals of 1939 earthquake (Ayetey and Andoh 1988).

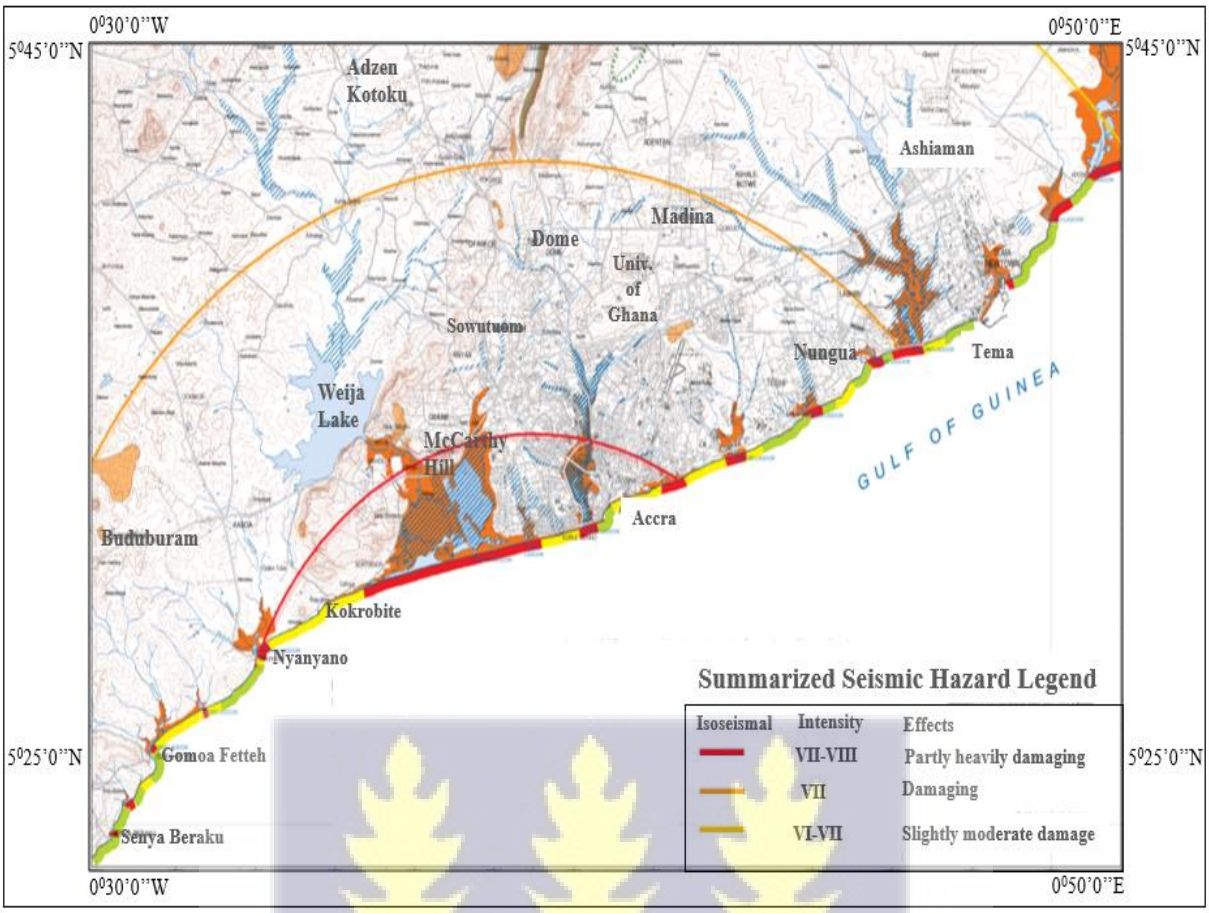

Figure 1.3 Current Geohazard map of Ghana (Source GSD 2010).

The impact of this and several relatively moderate size (MS 6 – 7) earthquakes around the world (e.g., Turkey, Haiti etc.,) has been extremely high because of construction errors and the poor soil conditions.

Therefore, without strict adherence to seismic criteria, there is a real risk of having the significant gains in development made so far within the GAMA, wiped out in the event of an earthquake. Seismic site effect distribution and soil classification is currently of critical importance for the GAMA.

Soil stiffness is a critical material parameter directly related to the load bearing capacity of structures on vulnerable soils. Consequently, when load capacity is underestimated for soils lacking sufficient stiffness, expected damage to structures during an earthquake is severe.

Shear wave velocity (Vs) and time-averaged shear-wave velocity to 30 m depth (Vs30) are key parameters in measuring important indices used in regional characterization of seismic site effect for robust PSHA and recommended standard earthquake engineering design (Aki, 1988; Boore et al., 1997; Borcherdt, 1970; Cramer et al., 2004; Frankel et al., 2009).

Recently developed surface wave geophysical techniques; ReMi (Refraction Microtremor) SASW (Spectral Analysis of Surface Waves) and MASW (Multichannel Analysis of Surface Waves) aimed at reducing the logistical and financial burden usually associated with traditional borehole studies (e.g., SPT, CPT etc.) have now become commonly used for geotechnical characterization of near surface (0-30 m) materials (Park et al., 1999; Xia et al., 1999; Xu et al., 1999; Miller et al., 1999, Stewart et al., 2003, Ivanov, et al., 2006, Park et al., 2007, Anbazhagan et al., 2009). They are non-invasive, less time-consuming, and well suited to intensely urbanized areas.

MASW is the most widely used surface wave technique. It identifies each type of seismic wave on a multichannel record, providing the highest signal-to-noise ratio.

MASW has been used in major earthquake geotechnical engineering, microzonation and site response studies to measure the dynamic properties of shallow soil. MASW, identifies subsurface material boundaries, and spatial variations in lithology from shear wave velocity (Anbazhagan and Sitharam 2008b; Ivanov et al., 2006; Rodríguez-Marek et al., 2001).

1.2 Problem Statement

The GAMA is seismically active and in recent times has experienced many impactful earth tremors, especially in the areas to the southwest of the region. There is a large accumulation of dynamic factors within this area, (faults, several impactful historical events, recent tremors) amidst a slew of bad construction practices, over population and poor planning, that render the area particularly vulnerable to earthquakes and its affiliated disasters on a daily basis.

Considering the very large logistical and financial effort to complete a soils conditions map using conventional methods, such as borehole studies, a detailed and regional soil conditions map necessary for structural engineering and improved earthquake hazard analysis for the GAMA, is yet to be completed.

1.3 Objectives

Main Objective

The study will measure regional quantitative and spatial distribution of site-specific seismic site effect response characteristics for the GAMA using multichannel analysis of surface waves

Specific Objectives

- The average shear wave velocity for various depths (Vs5, Vs15, Vs30, Vs40) will be mapped to evaluate the influence of topography on shear wave velocity over the tested area.
- Spatial heterogeneities of seismic response parameters will be compared and analysed using site classification criteria based on recommended site classifications scheme by the National Earthquake Hazards Reduction Program (NEHRP) scheme for the first 30 m of soil.
- Based on extensive geospatial database best site classification information that can be used for regional soil characterization and spatial zonation will be developed for the tested region.

1.4 Scope and Limitations

1.4.1 Scope

The study focuses on seismic hazard assessment involving site-specific investigations of shallow soils in a regional sense. The study uses *in situ* measurement of shear wave velocity

to assess soil stiffness for the GAMA with the MASW technique. In order to understand surface level response to earthquake ground motion, correlations between *in situ* data measurement of Vs30 (Shear wave velocity of upper 30m of soils) and surface geology as well as soil profiles in existing literature was compared.

1.4.2 Limitations

In most site classification studies using indirect surface wave techniques such as the MASW technique, measurements are correlated with direct measurements of the Vs profiles from borehole data at test sites. Though a large body of MASW data was collected for the study there is a very limited amount of reliable borehole data to properly constrain the measured data.

Additionally, distribution for the residual soils formed from the rocks that define the geology for the GAMA seem rather complex. Thus, it was difficult to pick up distinct variations with depth over the various geologic units. Data analysis has also been a major limitation since it was a challenge in acquiring a robust software for the analysis currently.

1.5 Study Area

1.5.1 Location and Size

The study is carried out over large areas covering the Ga East and West and parts of the Awutu Efutu Senya districts of the GAMA. The GAMA covers an approximate land area of 1550.37 km^2. The study area is bound by latitude 5°45'0" N and 5°25'0" N and longitude 0°30'0" W and 0°5'0"E (Figure 1.4)

The GAMA serves as the designated National Capital Territory of Ghana, with Accra being a very important hub of economic and administrative activities for the Greater Accra region and the outlining areas. Nearly 70% of the workforce employment in Accra is in the private informal sector. The metropolis is currently undergoing one of the fastest rates of urbanization, brought on by rapid in-migration, both from the countryside and also from other West African nations. A large portion of Ghana's GDP comes from Accra and attracts a large chunk of foreign direct investment into the country. Though it is the smallest region in Ghana with regards to land area, over 4 million inhabitants (projection from economic base of Accra, 2013),

live in Accra and it has become the second-largest metropolitan conglomeration in Ghana by population, and the eleventh-largest metropolitan area in Africa (Pescina, 2013).

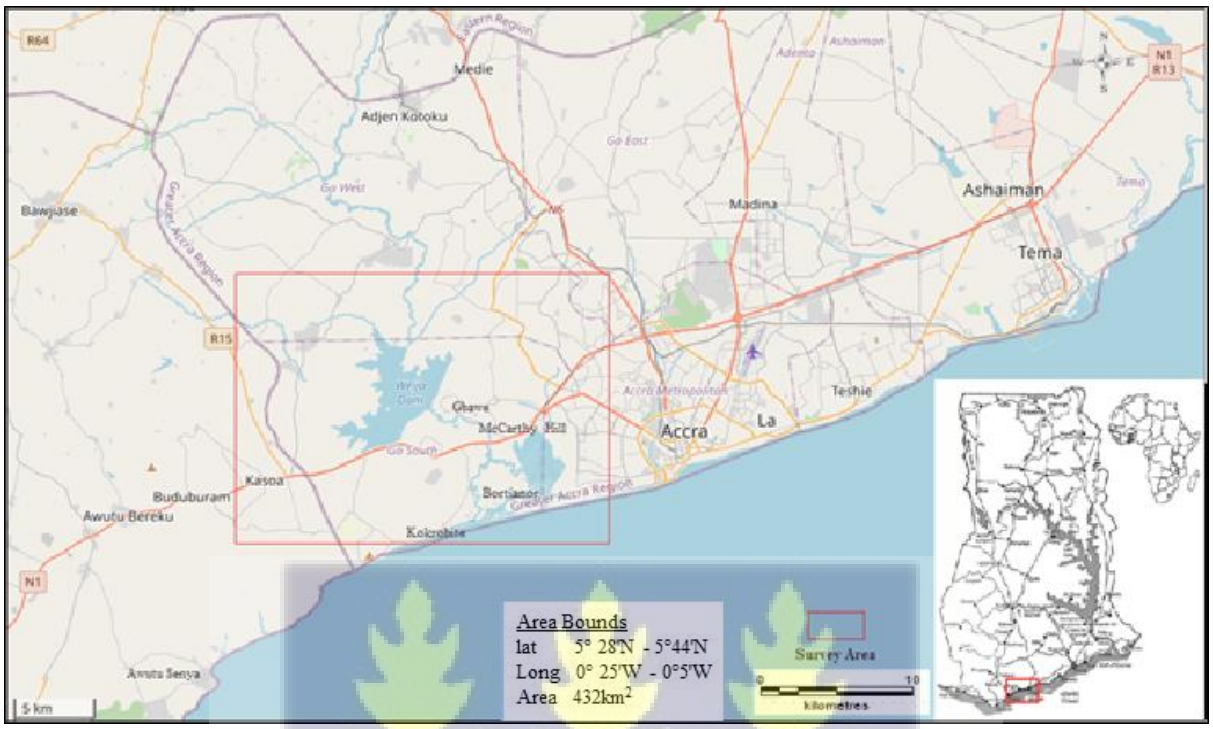

Figure 1.4 Map of the study area

1.5.2 Accessibility

A number of major first-class road networks lead out from Accra, connecting well to Tema, and major regions such as Ashanti Eastern, Volta and the Central regions of Ghana. The road networks throughout the metropolis are predominantly two-lane single carriageway, most of which are in relatively good condition. According to classification of Department of Urban Road, 45% of Accra roads are in poor condition. The primary road network in Accra radiates out from the central area (Accra Central – Kwame Nkrumah – Kaneshie Road corridor). Accra provides access to first class amenities, schools and hospitals.

1.5.3 Topography Geomorphology and Drainage

The geomorphology of the GAMA consists of four broad terrains namely the western lowlands, Akwapim Range, Eastern Lowlands, Coastal lowlands and Lagoons (Figure 1.5)

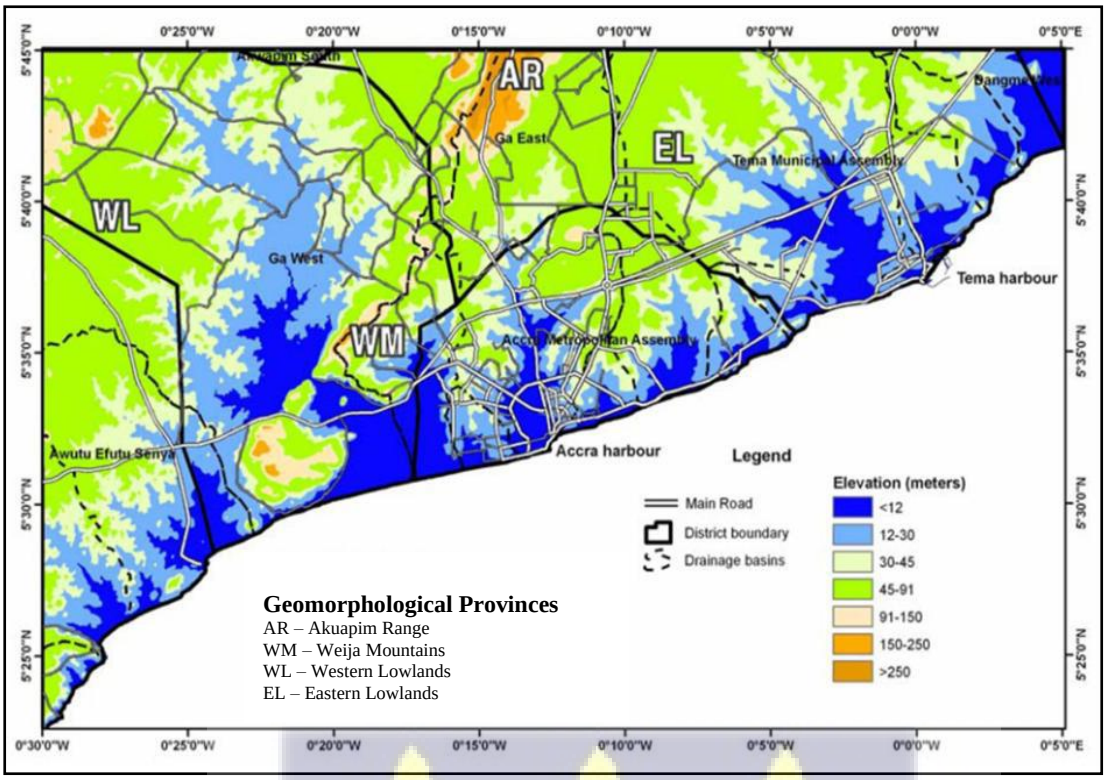

Figure 1.5 Geomorphological map for the GAMA (Source: GSD, Ghana-2012)

The Akwapim range is the highest elevation in the study area and distinctly separates the western from the eastern lowlands in the study area. The range generally trends northeast – southwest, rising to a height of 365 meters above sea level. Towards the east it is predominantly undulating, grading into the Accra plains. The Western Lowlands are low-lying with gentle rolling hills. The drainage system has a dendritic pattern and the rivers are perennial in nature. The drainage system is controlled by ridges and valley pattern of the topography. The Eastern Lowlands form a low-lying terrain with slope valleys. It has a very gentle gradient from the streams towards the ocean with a dendritic pattern forming the drainage system. The Coastal lowlands and lagoons comprise several sandy platforms with inlets and river deltas. These are usually flat unconsolidated sands having occasional interlayers of silt and clay. (Muff et al., 2006).

1.5.4 Climate

The study area falls within a tropical savanna climate that borders on a semi-arid climate. The GAMA experiences maximum rainfall in April to June and a minimum around September to October. Annual rainfall averages about 730 mm (MLG, 1992). Rainfall is short but intensive, usually triggering local flooding.

Annual average temperature is 26.8 °C. Because Accra's proximity to the equator, daylight hours are practically uniform during the year. Relative humidity is generally high, varying from 65% in the mid-afternoon to 95% at night. Temperatures are however generally cooler along the Akwapim foothills. (Muff et al., 2006).

1.5.5 Vegetation

Vegetation for the study area is a typical Savannah-type, characterized by three broad vegetation zones; shrub land, grassland and coastal lands. Dense clusters of small trees and shrubs occur more commonly in the western outskirts and in the north towards the Aburi hills. The coastal wetlands host dense grass, palms and coconuts trees. Agriculture within the metropolis is practiced in various basins with irrigated urban vegetable production being the most important type (Danquah, 2013).

1.5.6 Geological Setting

Paleoproterozoic (Birimian) provinces of the West African Craton generally lie to the west of the study area and the Dahomeyide orogenic terranes are to the east (Figure 1.6). These two terranes are separated by a major NE-SW tectonic boundary, where the rocks of the Dahomeyide orogens (Akwapimian-Togo belt) are thrust westward onto the eastern margin of the West African Craton. The Dahomeyan, defines the basement on which the cover rocks within the Dahomeyide lie. They are composed of metamorphosed Precambrian rocks (Quartz

schist, Orthogneiss, Metamicrogabbro, Amphibolites and Schistose Marbles). The Togo Structural Units include granitoid and biotite gneisses, mica schist and thickly bedded sandstones. Their occurrences are restricted to the coastal zone and they are present on- and offshore. The sediments of the Accraian basin possess a Devonian age and are discordantly overlying Neoproterozoic Togo rocks. The centre of Accra lies on the Devonian shales and interbedded sandstones with the sandstones becoming massive at the base (Ayetey and Andoh 1988). Those sediments, whose beds are slightly folded and dip generally towards the south at angles between 5^0 and 25^0, are considerably faulted with a rather complex structure.

1.5.7 Soil

According to Ayetey and Andoh (1988), bedrock, topography and drainage control the type and distribution of the soils within the study area. The soils found in the low flat lands within the Accra are predominantly clays and sands. Typically, the interbedded sandstone and shale formation of the Accraian gives rise to fine to coarse sands in low lying areas, turning silty to clayey where shales are interbedded. On higher ground where drainage is good, sandy to gravelly lateritic soils are prevalent.

The shale series in this formation generally result in clays.

The Togo series generally form fine to coarse sands in low lying areas grading through gravelly laterites to highly quarzitic cobbly to gravelly laterites on high ground.

The schist zones form clayey to silty sands. The Dahomeyan gneisses give rise to heavy clays and silty- sandy clays in valleys and river courses. In higher ground the clays become lateritic with development of gravel.

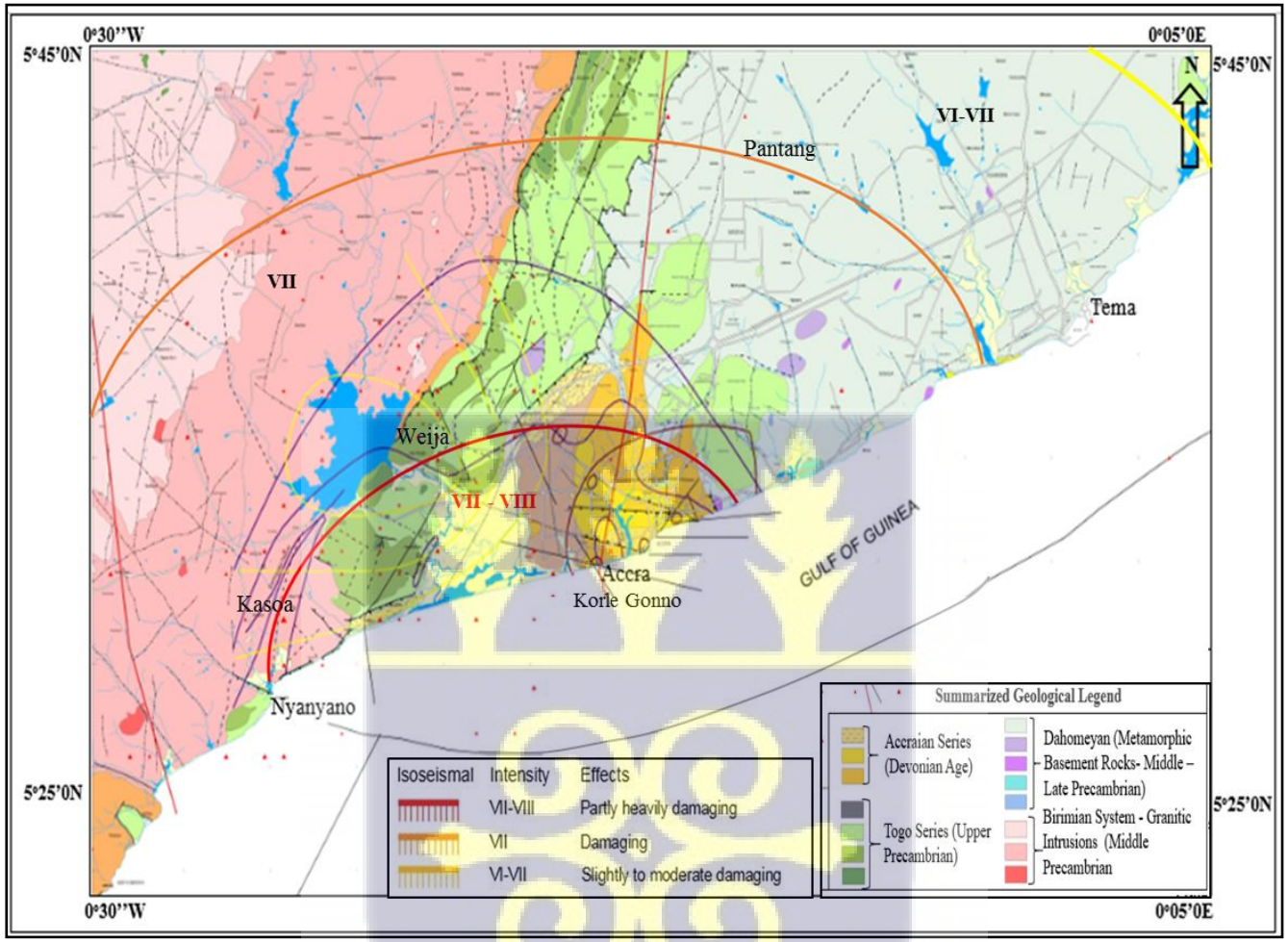

Figure 1.6 Geology Map for Study Area (Source: GSD, Ghana-2012)

CHAPTER TWO

LITERATURE REVIEW

2.1 Seismicity and the Tectonoseismic Elements of the GAMA

The 1939 earthquake has been the most impactful earthquake in Ghana, till date. The epicentre of this and numerous recent seismic occurrences (ML3.8-4.8; 1997, 2003, 2008, 2011, 2012, 2020) is located within the tectonoseismic region of Ghana, located west of Accra, where the Akwapim fault zone intersects with the coastal boundary fault. (Figure 2.1).

There are many views about the cause of the seismicity in Ghana's seismic regions. Previous studies have generally correlated seismic events with the tectonic elements that are defined for the in south of Ghana (Tevendale, 1957; Burke, 1969b; Bondesen and Smit, 1972; Ahmed et al., 1977).

2.1.1 The West African Craton

Ghana is situated on the West African Craton's south-eastern edge (WAC). At the end of the Eburnean orogenesis, about 2000 Ma ago, the West African Craton (WAC) became tectonically stable (Camil, 1984; Yacé, 1984; Black, 1985). The craton is completely encircled by Pan-African belts, which indicate the end of the Eburnean orogeny's last stages.

The West African Craton defined for Ghana's seismic regions is made up of passive margin sediments deposited in the Volta basin at the WAC's SE boundary as a result of several extensional events associated with continental breakup suffered by the WAC at the start of the Neoproterozoic, as well as the basement terranes of the Proterozoic Birimian provinces of the WAC. The Birimian encompasses around two-thirds of Ghana's land area (Ahmed et al., 1977, Ako & Wellman 1985; Ne´de´lec et al. 2007).

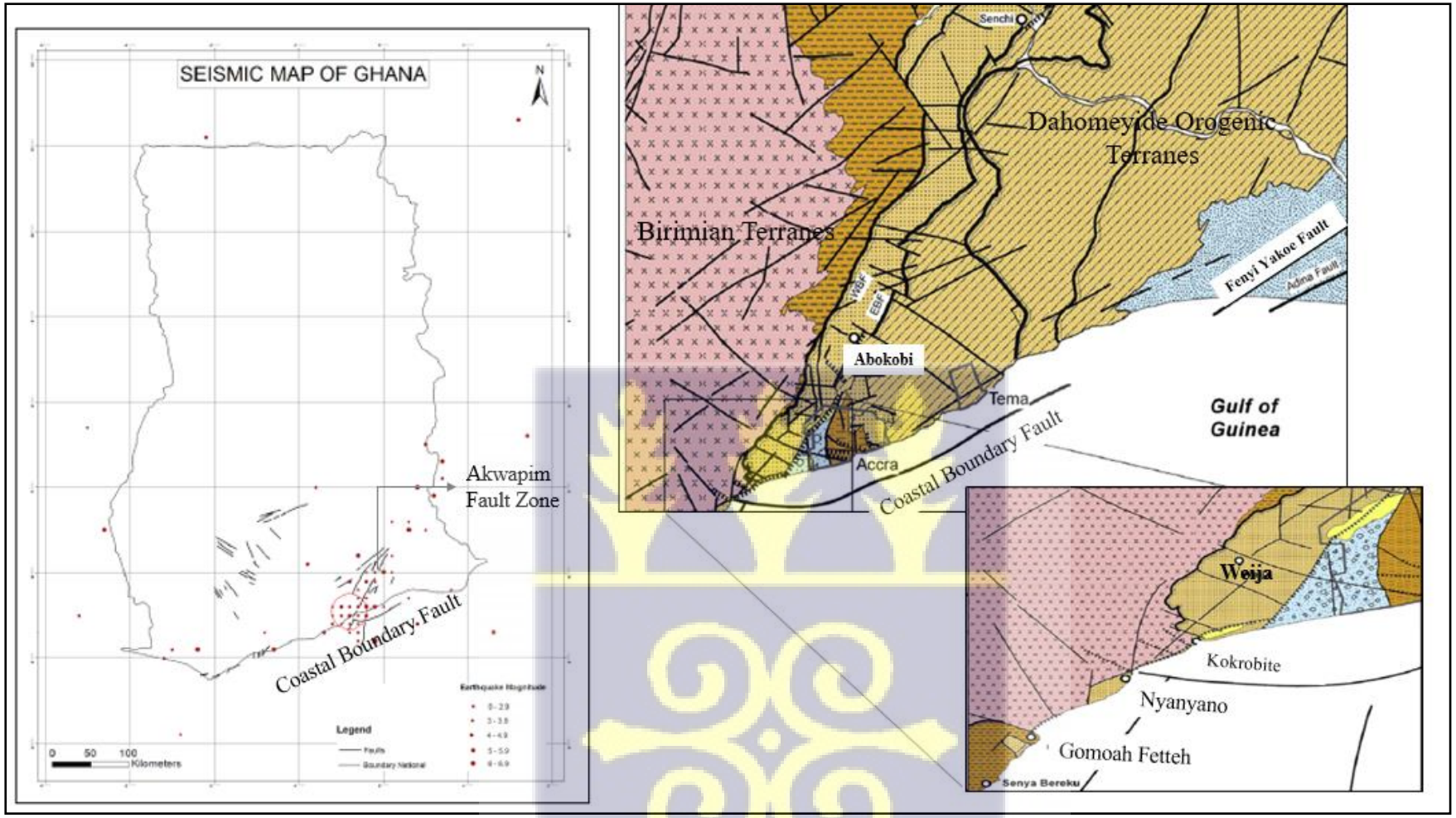

Figure 2.1 Map of southeastern Ghana showing major tectonic elements in Ghana's seismic regions (after EERI 2015 report, GSD, BGR 2009 and from Muff and Efa 2006)

2.1.2 The Pan-African Orogeny

The Pan-African describes Neoproterozoic to Palaeozoic tectonic, magmatic, and metamorphic activity. In Africa, the Pan-African orogeny entails the creation of multiple orogenic mobile belts that surround the older WAC (Trans-Saharan belt, Pharuside, Anti-Atlas, Bassaride, Rockelite, Mauritanide, and so on). The closing of numerous major Neoproterozoic oceans, as well as a series of subduction and collisional orogenics involving various tectonic settings, led in the formation of a network of mobile belts (Trompette, 1997 and Caby, 2003).

The southwestern segments of this Trans-Saharan comprise the Dahomeyide orogen. The Dahomeyide is exposed in south-eastern Ghana, parts of Togo and Benin where it is interpreted to have resulted from the easterly subduction of the rifted margin of WAC (Affaton et al., 1991; Agbossoumondé et al, 2004; Attoh and Nude, 2008). The Dahomeyide is sutured onto the WAC as evidenced by nappe stacking and crustal imbrication (Affaton et al., 1991, Caby 1987, Attoh et al., 1997, and Agbossoumondé et al., 2001).

The Pan African Orogeny began in Ghana when the Birimian rocks, which began in a previous orogeny about 2.1 Ga ago, became the basement rock to a sedimentary cover sequence; the Akwapim Togo belt. Within the orogenic zone, the cover was strongly folded and thrust on south-easterly dipping planes, was lightly metamorphosed and perhaps locally subjected to granitization and to granite intrusion, while the Birimian basement was reactivated to give the unit known as the Dahomeyan (Ajibade and Wright, 1989, Caby, 1989; Affaton et al., 1991, Castaing et al., 1993;). The Dahomeyide Orogen generally occupies the eastern part of Ghana's seismic region.

It is separated from the basement Birimian on the west by a major NE-SW tectonic boundary, along which the metasedimentary Akwapimian cover sequence is thrust westward onto the eastern margin of the West African Craton

2.1.3 Sedimentary Basins and Faults in the Coastal Zone

The Accraian formation is mostly found in Accra's central capital district, up to the outskirts of the airport to the east. It can be found as a fossiliferous succession of alternating Devonian shales and interbedded sandstones.

The formation is folded and faulted (McCallien, 1962), with those sediments, whose beds slightly folded and dipping generally towards the south, being considerably faulted with a rather complex structure (Ayetey and Andoh 1988). The Basin is tectonically closed, by the Dahomeyan System to the east and northeast and rocks of the Togo formation to the west and northwest (McCallien, 1962, Fitches 1970, Kesse 1985).

Recent studies (unpublished data, Quaah, 2013) concluded that the Coastal boundary fault (CBF) has been one of Africa's most active faults over the last 500 years. It stretches for about 25 kilometres offshore and along Ghana's entire coastline, from Half Assini to Denu. It bends west of Accra to strike east west and intersects the Akuapim Fault Zone (AFZ). According to Blundell (1976), the CBF forms the northern margin of the Keta Basin.

The Romanche fracture zone (RFZ) has been established, as a series of NE-SW-trending east-dipping transpressional structures that occur at the eastern side of the Mid-Atlantic and the Romanche Transform and Fracture zone (Blundell and Banson, 1975, Akpati, 1978, Bacon and Quaah, 1981; Attoh et al., 2004, 2005). It represents an inactive transform fault of the Mid-Atlantic Ridge which separates the continental from oceanic crust of West Africa and Ghana (Deltail et al., 1974; Mascle and Sibuet, 1974; Edwards et al., 1997; Attoh and Brown, 2008). Previous studies mention that the RFZ makes presence on shore in Ghana near Goi- Sege some 100 km east of Accra (Pichon and Hayes 1971), however observations by Antobreh et al. (2009) from seismic reflection studies provide evidence to the contrary. The authors rather refer to the Akuapim Fault Zone (AFZ) as splays of the Romanche Fracture Zone instead of continental extensions.

The seismicity of southern Ghana has been linked with movements along the AFZ and the Coastal Boundary Fault a few kilometres offshore (Burke, 1969a, Blundell, 1976, Sykes, 1978, Bacon and Quaah, 1981, Quaah, 1982).

The Akwapim fault zone is NNE striking system of faults defined by two Neoproterozoic age overthrusts west and east. These are referred to as the Western Boundary Fault (WBF) and Eastern Boundary Fault (EBF) respectively (Ahmed et al., 1977).

Studies on the focal mechanisms, source parameters and the historical seismicity of Ghana, converge on the fact that there have been more activities along the Akwapim fault zone. The facts further indicates that, seismic activity and shearing effects, diminish with distance from the continent–ocean boundary (Burke, 1969b, Bacon and Banson, 1979, Bacon and Quaah 1981, Attoh, 2004). However, ideas on the source of seismicity are varied.

2.2 Recent Seismicity and Seismic Hazard Assessment for the GAMA

Since the 1939 earthquake, the GAMA has been subjected to several earth tremors with magnitudes ranging from 0.4 to 4.8. Since 1997 these small tremors have increased in frequency with events occurring in 2003, 20l8, 2011, 2012 and, 2020. The impact of these were felt significantly in the west of Accra. There are several positions on what caused recent tremors felt in the metropolis and its immediate surroundings.

Several studies after the 1970's (Blundell and Banson 1975, Mascle and Blarez 1987, Blarez and Mascle 1988, Attoh et al. 2004, Basile et al.2005 and Antobreh et al. 2009) have established several evidences of occurrence of neotectonic normal faults, controlled by pre-existing structures and lithological inheterogeneities in the crust as cause for recent seismic activity. These faults show very variable strike directions along the Pan-African rocks. Burke (1969a) provided evidence of downthrow (≈ 400 m) of the lowlands to the East of the Akwapim Togo Belt in Quaternary times (Figure 2.2), from topographic analysis and the interpretation of a drillhole near the settlement of Abokobi at the foot of the Akuapim range. Muff and Efa, (2006) mentioned unconsolidated talus conglomerate and slope talus marks, found NE of Kokrobite in the coastal area and the southernmost section of the EBF as evidence of fault-lines for ENE–WSW striking neotectonic normal faults in the Nyanyano–Kokrobite area. Some authors (Blundell and Banson 1975, Attoh et al. 2004 and Antobreh et al. 2009) have also described a complex horst and graben system where evidence of Quaternary subsidence on many normal faults in the shelf area are observed. Ghana's margin subsides as a normal passive margin beneath the heavy ocean floor. The shearing effects diminish with distance from the continent–ocean boundary (Attoh et al., 2005). The structural evidence detailed suggest that the several neotectonic high-angle style normal faults projected in the shelf and

coastal area resulted from shearing, triggered on the Ghana's continental margin, as the ocean floor is dragged down (Figure 2.2).

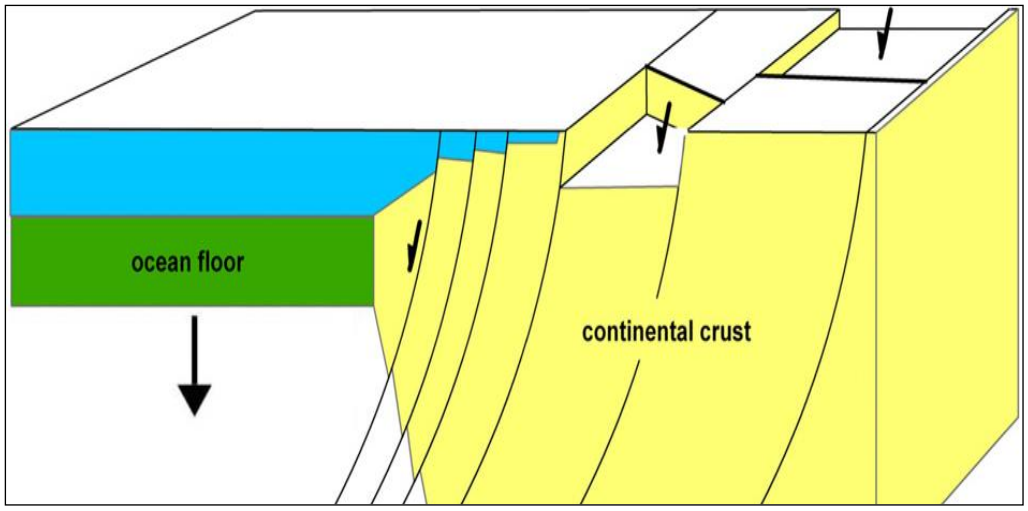

Figure 2.2 A model for seismic events in southeast Ghana showing down-sagging of heavy ocean floor causing normal faulting in the coastal area (after Amponsah et al., 2012).

There is as yet no detailed soils conditions and seismic site effect response map currently covering the GAMA. Projections for ground acceleration and other seismic coefficients for sound seismic engineering have been referenced from overseas building codes (EERI Housner Report 2015).

Because regional differences in geotechnical properties are not addressed when using these generic seismic criteria found in these building codes, real ground motion can be miscalculated (Kim et al. 2002). Due to variances in regional and geological ground conditions, major study results have recently revealed differences in seismic response characteristics (Lee et al. 2012). Building codes such as the Uniform Building Code (UBC) and the International Building Code (IBC) and all associated derivatives, were derived mostly from empirical seismic readings, damage data or numerical analyses from the western United States, (Dobry et al. 2000; ICC 2000, 2006).

Just like the GAMA, and many other seismic regions around the world, variances might occur, because the US region used in developing these codes have deeper bedrock and stiffer soils

(Sun et al. 2005), and thus may not be well suited for their particular geological setting. Terrain and geological factors play a role in these geotechnical qualities (Wills et al. 2000; Wald and Allen 2007). Major sites in the western United States are primarily constituted of vast plains with simple geological conditions. The GAMA's soil distribution is complicated, with heavy silty sandy-clays or fine to coarse sands at lower elevations and a variety of lateritic type soils at higher elevations (Ayetey and Andoh, 1988). Unconsolidated sand and clay deposits define low-lying coastal locations like as Accra, Nyanyano, Sakumono, Korle Gonno, Aplaku, Tetegu, and Weija.

Changes in topography or subsurface geological conditions are closely linked to region-specific geotechnical characteristics and are therefore regarded as additional amplification factors that must be ignored in site investigations, especially for seismic hazard assessments. In circumstances of substantial earthquake damage, such further amplification factors have also been documented (Green et al. 2011). As a result, in the event of any seismic occurence due to amplifications caused by intrinsic characteristics of regions and locations, quantitative assessment of geotechnical parameters must take precedence.

Seismic hazard analyses involves the quantitative estimation of ground-shaking hazards or ground failure at a particular site weighted against its associated effects on human activities (Anbazhagan and Sitharam, 2009).

Depending on the seismic environment or scope of the project (i.e., single site or a region) the approach used may be deterministic (a particular earthquake scenario is assumed) or probabilistic (uncertainties in earthquake size, location, and time of occurrence are explicitly considered) in nature. Both methodologies are meant to complement one another to provide additional insights to the seismic hazard problems, the overall aim is to provide useful

parameters to influence proper land-use planning, engineering design, and ultimately seismic risk mitigation.

Since an extensive database of accelerograms with similar source, path and site conditions is not yet available, all the seismic hazard maps produced for Ghana so far have been deterministic in approach. Peak ground acceleration proposed for the GAMA is between 0.14 g - 0.57 g (Amponsah et al., 2008). The subsequent use of different values for peak ground accelerations (BRRI 1990 or IBC 2006) values) used by Ghanaian engineers has called for the development of a robust probabilistic seismic hazard analysis even with the limited available data, using current available systems developed in recent times.

The inclusion of a general regional distribution of site-specific conditions in seismic hazard assessments, has been recommended as an adequate representation of the seismic hazard. The damage to structures during earthquakes reflects the underlying subsoil conditions.

The geographic distribution and intensity of the damage are strongly affiliated with local lithology; physical properties (e.g., silt and clay content, as well as void ratio) and importantly conditions of the near-surface sediments. Local geological conditions may generate significant amplification of ground motion and concentrate damage during an earthquake.

The average shear-wave velocity over the first thirty-meter depth (Vs30), of soil is currently the standard parameterisation for addressing site-conditions in building codes in several current studies (e.g., Park and Elrick, 1998, Dobry et al., 2000, Montalvo-Arrieta et al., 2002, Stewart et al., 2003, Holzer et al., 2005, Kanli et al., 2006, Tokeshi et al., 2013). Vs30 is the primary parameter of choice also in the development of ground-motion prediction equations (e.g., Boore et al., 1997, Boore and Atkinson, 2008) as well as, addressing the applicability of the predictive equations outside the region that provided ground motion data, (Vilanova et al., 2012).

GAMA soils distribution is generally complex with heavy clays, silty-sandy clays and fine to coarse sands, mostly at lower elevations (valleys and river courses), which grade to a range of gravely or highly quartzitic cobbly lateritic soils on higher ground. The sandstone series of the Accraian formation however are rather fine to coarse sands in low lying areas, turning silty to clayey where shales are interbedded. Similar to the Dahomeyan and the Togo series, lateritic soils are prevalent on relatively higher ground where drainage is good (Ayetey and Andoh 1988). These soft soils are prone to significantly amplify seismic waves triggering liquefaction and cause significant damage especially in the low-lying areas close to the coast in and around Nyanyano, Korle Gonno, Aplaku, Tetegu, Sakumono lagoon Weija and Fete and Accra near Christianborg castle (Junner et al., 1941, Ayetey and Andoh 1988).

2.3 Multichannel Analysis of Surface Waves

The frequency dependent characteristics of Rayleigh waves has in recent times become a useful tool in the development of several non-invasive surface techniques; Spectral Analysis of Surface Waves (SASW, Nazarian and Stokoe, 1983), Multichannel Analysis of Surface Wave (MASW, Park et al., 1999), Refraction Microtremor (ReMi, Louie, 2001) etc. They are generally non-invasive and have been successfully used in the determination of shallow shear-wave velocity and the dynamic properties of shallow soils.

Invasive methods such as Standard Penetration (SPT) test (Youd et. al., 2001), Cone Penetration (CPT) test (Robertson & Wride 1998) and Dilatometer (DMT) testing, are usually time consuming, costly and not particularly well suited to intensely urbanized areas.

Surface wave techniques (highlighted above) thus, provide less expensive and time efficient alternatives, which allow large (urban) areas to be covered while still attaining a reasonable depth of investigation. Seismic refraction method is conventional in mapping near-surface structures. It is the oldest and most extensively practised non-invasive near-surface seismic method. Seismic refraction is commonly preferred for investigations either in areas where the geology is not particularly complex or in places where the objective is to map the top of bedrock. However, it is majorly handicapped by the assumption of increase in velocity with depth and tends to give erroneous results when complex geological terrains (dipping or discontinuous layers, low velocity layers where a sand layer underlies a clay layer, or very thin layers) are encountered in near-surface studies. Here the Rayleigh waves, the principal component of ground roll appear as dominant events in seismic records and is considered as 'noise'. Consequently, a considerable large amount of time is spent in trying to remove those signals.

The best alternative offered in recent times are the surface wave techniques (e.g. SASW, MASW and ReMi). These techniques are primarily favoured for their precision and swiftness to estimate the subsurface shear wave velocity profile over a large area. Some studies have shown the effectiveness of these techniques in the estimation of dynamic properties of shallow soils, mapping and identification of anomalous material and the presence and location of voids and karst features, in complex geological terrains and even in noisy environments (e.g. Miller et al. 2000).

SASW (Spectral Analysis of Surface Waves) and MASW (Multichannel Analysis of Surface Waves) are the most widely used amongst all the surface wave techniques. While both techniques involve the use of an impulsive source to generate records, the SASW uses only a pair of receivers, making the evaluation and differentiation of signal from noise difficult. To overcome these inherent challenges, the MASW incorporates multichannel analysis of the surface wave (Park et al., 1999; Xia et al., 1999; Xu et al., 2006).

Spectral Analysis of Surface Waves (SASW) is the earliest of the surface wave techniques developed to generate the near-surface Vs profile. It was introduced by Nazarian and Stokoe in the early 1980's (Xia et al 1999). The technique essentially makes use of the spectral analysis of ground roll generated from active source seismic energy, involving a field procedure which utilizes only two receivers (geophones). Although it was favoured for its simple field test configuration and the straightforward theory behind it, because repeated testing using several testing configurations was required just at one test site so as to attain the targeted range of investigative depth, invariably the entire process rendered it rather laborious and time consuming. Additionally processing of data requires subjective judgments that sometimes influenced the final results, as the method assumes that the most energetic arrivals are Rayleigh waves. Thus, where noise overwhelms the power of artificial sources such as in urban areas or

where body waves are more energetic than Rayleigh waves, SASW yielded unreliable results (Brown, 1998; Sutherland and Logan, 1998).

Multichannel Analysis of Surface Waves (MASW) was developed by Park et al., (1999) in response to the shortcomings of SASW. One of the major strengths in the technique is the statistical redundancy to measurements of phase velocities given by the simultaneous recording of up to 24 receivers at short (1 m - 2 m) to long (50 m -100 m) offset distances from an impulsive or vibratory source. Multichannel data displays in a time-variable frequency format. The setup allows identification and rejection of non-fundamental-mode Rayleigh waves and other coherent noise from the analysis (Louie, 2001).

MASW has been successfully used in many studies to attain *in-situ* shear wave (Vs) velocity profiles (Park et al., 1998a, Xia et al., 1999, 2003; Kanli et al., 2006; Anbazhagan and Sitharam, 2008a, Anbazhagan and Sitharam 2008b, Tokeshi et al. 2013) to characterize subsurface conditions.

Surface wave inversions are solved indirectly through either, a deterministic optimization approach, based on least-squares method (Xia et al., 1999) or random approach (Socco and Boiero, 2009) or a combination of both. The objective at this stage is to obtain accurate dynamic earth properties from surface wave data (measured field records, dispersion curves etc.). Accurate determination of shear wave velocity (profiles) gives a direct indication of the shear and Young's moduli which are associated with the material's stiffness and load bearing capacity of the ground

Basic inversion is based on the fundamental principle that the fundamental mode (M0) dominates the field records. Constructed M0 curves are matched to the earth's Vs structure whose theoretical M0 curve most closely matches constructed M0. The root-mean-square (RMS) error is usually used as an indicator of the closeness between the two dispersion curves

(measured and theoretical), and the final solution with the least RMS error is chosen as the 1D Vs profile. 1D model (S-wave velocity vs. depth) inversions represents shear wave variations with depth through the lateral averaging of the subsurface material for the entire surface distance covered (one 1D Vs profile is generated from each curve).

The fundamental mode inversions have the inherent problem of non-uniqueness (i.e. mode misidentification and mode-mixing), thus multimodal inversions which includes higher-mode curve(s) for the inversion provides more accuracy (resolution) of the final 1D Vs profile.

Dispersion image and raw data inversion approaches (Ryden and Park, 2004; Forbriger, 2003) address the drawbacks of modal-curve-based inversions by avoiding the extraction of modal curves. Dispersion image inversions use dispersion image data (i.e., phase velocity spectra), while the raw data inversion eliminates the bias caused by subsequent data processing such as dispersion imaging or curve extraction by using the raw multichannel field record as it is without any further processing such as dispersion imaging.

CHAPTER THREE

METHODOLOGY

Ground roll data was collected over 84 lines at forty-two (42) locations within the GAMA, for the study. Two (2) intersecting lines oriented approximately E-W and N-S were proposed over each test site.

The general procedure for estimation of shear wave velocity data up to 30 m depth, from inversion of fundamental mode dispersion curves for the study is detailed below;

- Preliminary site visits were conducted to determine suitability of site for conducting effective MASW survey. Layout and placement of MASW lines were subsequently established (Figure 3.1 a). Unsuitable sites such as those highlighted in figure 3.1 b were exempt from the study.
- Collection of active MASW shot gathers.
    - 42 locations established
    - Station Spacing : 2 m
    - Source: 8 kg sledgehammer (3-5 impact stack)
    - Receivers: 4.5 Hz geophones (18 active receivers available for use)
    - Recording: 24 channel (1 SmartSeis ST Geode)
    - Shot interval: 2 m
    - Source offset :12 m
    - Receiver Spread 36 m
    - Number of shots per spread 7 shots
    - Number of spreads 3
- Dispersion Curve Analysis
    - Extracting dispersion curve

- Estimating the fundamental-mode dispersion curves
- Inversion of fundamental mode dispersion curve to obtain 1D, 2D (Vertical and surface) profiles

3.1 General Acquisition Parameters Logistics and Site Conditions

For optimum data acquisition of ground roll, the geometry and field survey parameters modified according to Park et al. (2001), illustrated in Figures 3.2(a) and (b), below, were used. A 24-channel seismograph (SmartSeis ST System) was used to record and store ground roll for processing.

Typically, twelve (12) or more geophones are utilized. Geophones are arranged equidistant from each other. Each geophone is connected to its own recording channel (see figure 3.1 a). The number of geophones utilized in most surveys, if available, is typically between 24 and 48. (e.g. Donohue, Dermot & Donohue, 2013; Lin, Chang & Lin, 2004; Park & Carnevale, 2010).

In general, a better resolution in the dispersion image is produced by increasing the number of geophones employed for recording (Park et al., 2001; Ryden, Park, Ulriksen & Miller, 2004).

Eighteen (18) vertical geophones of 4.5 Hz capacity were available for use in the current study.

In MASW surveys, a recording frequency (fs) of 1000 Hz is most typically employed. This corresponds to a 1 millisecond sample interval (dt).

The overall recording time (T) for MASW surveys using an impulsive seismic source is typically approximately 1 second. For a large receiver spread (D > 100 m), a longer recording duration (e.g. T = 2 seconds) is advised (MASW, n.d.a.). A longer recording duration is necessary for directly collected swept-frequency recordings, i.e. surface wave records generated by a vibrating seismic source (Park et al., 1999).

For the study a total recording time of 1000 ms (1sec), with 1 ms sampling interval and record length of 2 seconds was used. In order not to cause the signals generated to be attenuated prematurely, especially at the far end of the array, no acquisition filters were used for the current study.

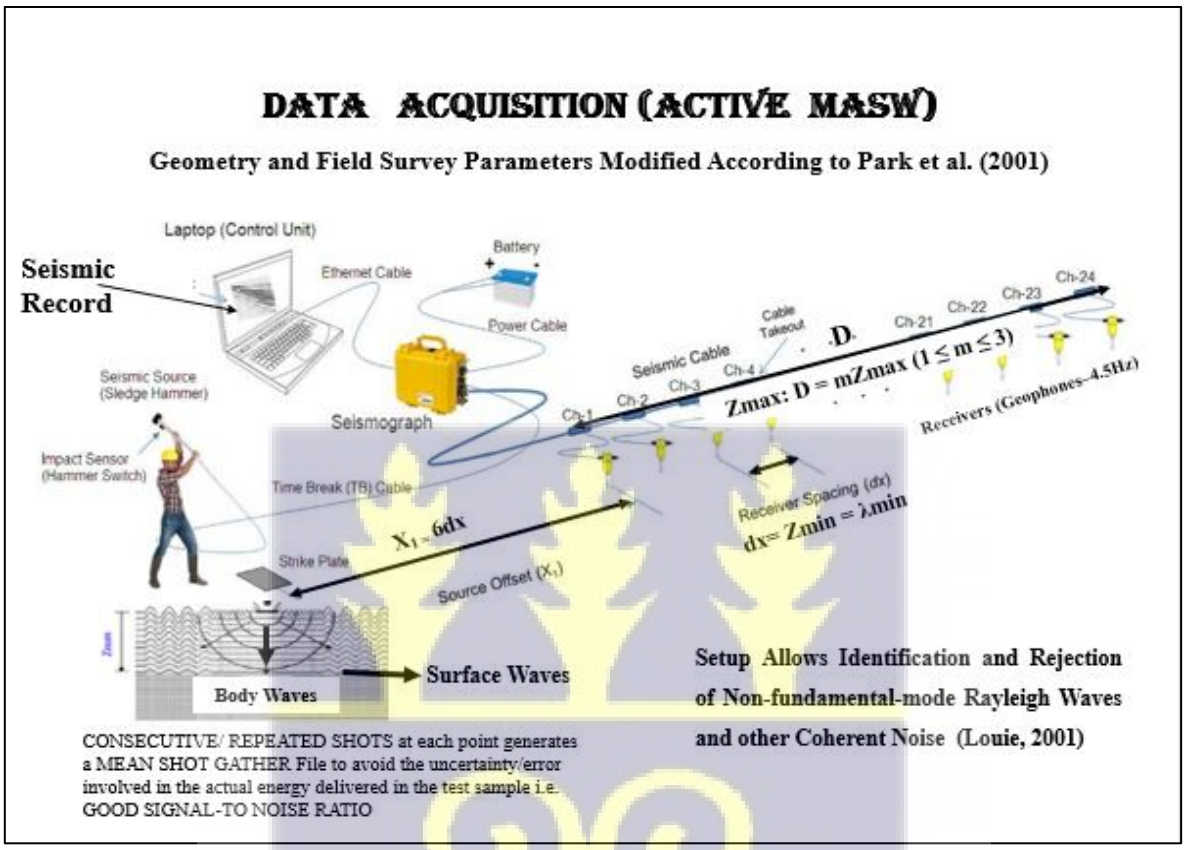

Figure 3.1a Basic layout of MASW field survey (after Park et al. 2001)

Figure 3.1b Field logistics for general linear array setup for MASW survey

The longest depth of investigation (Zmax) varies depending on the location and kind of seismic source. The largest surface wave wavelength acquired during data capture (λmax) determines the maximum desired depth of investigation (Park & Carnavele, 2010);

$$Z_{max} \approx 0.5\lambda_{max} \quad \text{.....Eq. (1)}$$

In keeping with recommendations by Richart et al. (1970), Gucunski and Woods (1991), and Stokoe et al. (1994), each spread was kept at 36 m (long enough) to avoid far field effects. The length of the receiver spread D represents the distance between the first geophone and the last geophone (geophones are arranged equidistant from each other). This length (D) is directly related to the longest wavelength (λmax) that can be analysed;

$$\lambda_{max} \approx D \quad \text{.....Eq. (2) or}$$

$$Z_{max} \approx 0.5D \quad \text{……...……Eq. (3)}$$

If longer wavelengths than Eq. 2, is desired for investigations, there is a real risk of achieving less accurate results. Thus, the optimum receiver spread length has been suggested to lie within the range of;

$$Z_{max} \leq D \leq 3z_{max} \quad \text{.....Eq. (4)}$$

When D is excessively long, surface waves generated by most common seismic sources become attenuated below noise level at the end of the receiver spread (far field effects). Consequently, the signal from the furthermost receivers is usually too noisy to be usable (MASW, n.d.a.; Park et al., 1999).

Receiver spacing (dx) for the study is 2 m and represents the shallowest resolvable depth of investigation Zmin. This determines the shallowest resolvable depth of investigation (MASW, n.d.a);

$$dx = n \cdot Z_{min} \text{ where } 0.3 \leq n \leq 1.0 \quad \text{Eq. (5)}$$

Source offset (x_1) is the distance between the source and the nearest receiver. For the study, x_1 was placed 12 m away from the first geophone. This distance was far enough to minimize near field effects (not fully developed surface waves being picked up by the nearest geophones) and far enough, for the planer characteristics of R-waves to be apparent. Near-field effects have the tendency to lead to underestimated phase velocities and decreased investigation depth in MASW surveys (Park & Carnavare, 2010).

As a general rule of thumb;

$$x_1 = 6dx \quad \text{Eq. (6)}$$

or

$$x_1 \geq 0.5D \text{ where } \lambda_{max} \approx D$$

Equation 7 suggest minimum and maximum source offsets that can be used for effective surveys (MASW, n.d.a.);

$$x_{1,min} = 0.2D \text{ and } x_{1,max} = D \quad \text{Eq. (7)}$$

Essentially long source offsets ($x_1 \geq D$), may enhance energy for long-wavelength surface waves, and consequently increase λmax for a given receiver spread (Park & Carnavare, 2010),

however, this will invariably result in lack of short-wavelength wave components due to excessive attenuation (Park & Shawver, 2009).

Topographical conditions also have some effect on the quality of the recorded surface wave data. It is recommended that receivers are placed on relatively flat terrain (See Figures 3.1 b). Surface reliefs within the receiver span greater than around 0.1D can have significant effect on the surface wave generation (Figure 3.2).

Also the slope of the surface along the receiver span can affect the accuracy of the resulting dispersion curves. Where the slope of the topography along the receiver span is less than 10°, dispersion characteristics can be estimated with less than 4% error (Zeng et al. 2012).

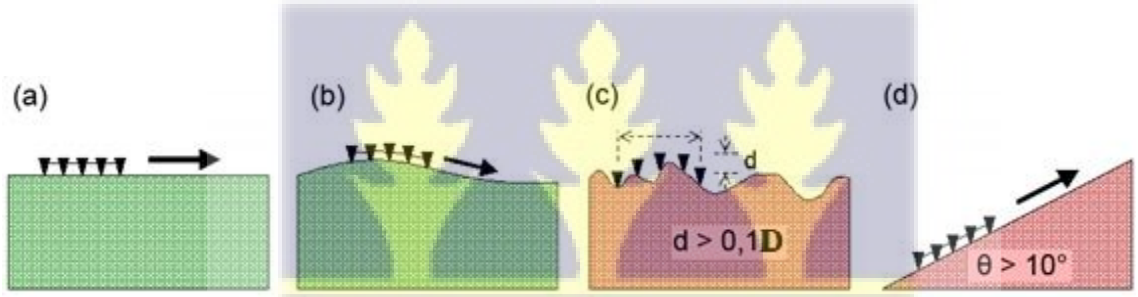

Figure 3.2 Topographical conditions and quality of multichannel surface wave data, based on MASW (n.d.a).

Generally, a heavier seismic source ensures a deeper depth of study. A reasonably heavy sledgehammer (e.g., 10 kg) is a common choice, which can result in an investigation depth of 10-30 m. Surface waves of lower frequencies (longer wavelengths) can be created by a source capable of delivering more impact power into the ground, such as a crane and a large falling load, allowing the required depth to increase below 30 m. The use of a metallic or non-metallic impact plate (base plate) can also aid in the generation of lower frequency surface waves. A metal plate is a more traditional option. However, it has been observed that utilizing a firm rubber plate, is feasible to create surface waves with significant lower frequencies (MASW, n.d.a.).

For this study, a sledgehammer (≈ 8 kg) connected to the seismograph through a hammer cable was used to strike a 300 x 300 mm steel plate to generate (R-waves) surface waves.

Depending on site conditions, multiple (3-10) shot records were stacked at each shot location to obtain mean shot records with improved signal-to-noise ratio. Shots were gathered under unique file names and stored as SEG-Y data format on the 24-channel seismograph for fundamental mode dispersion curve identification and analysis.

3.2 Data Processing for 2D Analysis and Interpretation

2D velocity models used for the study obtained by;

i. Loading the SEG-Y data file in Easy MASW software.

ii. Creating geometry.

iii. Generating dispersion image of the Rayleigh waves.

iv. Picking the fundamental mode dispersion curve (one curve each from a total of 13 records).

v. Inverting to obtain S-wave velocities and 1D (depth) Vs profiles using extracted dispersion curve (back-calculating Vs variation with depth that gives theoretical dispersion curves closest to the extracted curves, one 1D Vs profile is generated from each curve).

vi. Stacking of multiple 1D results into 2D images

2D models used in the study are generated using the generalized 2 step scheme illustrated in figure 3.3 below;

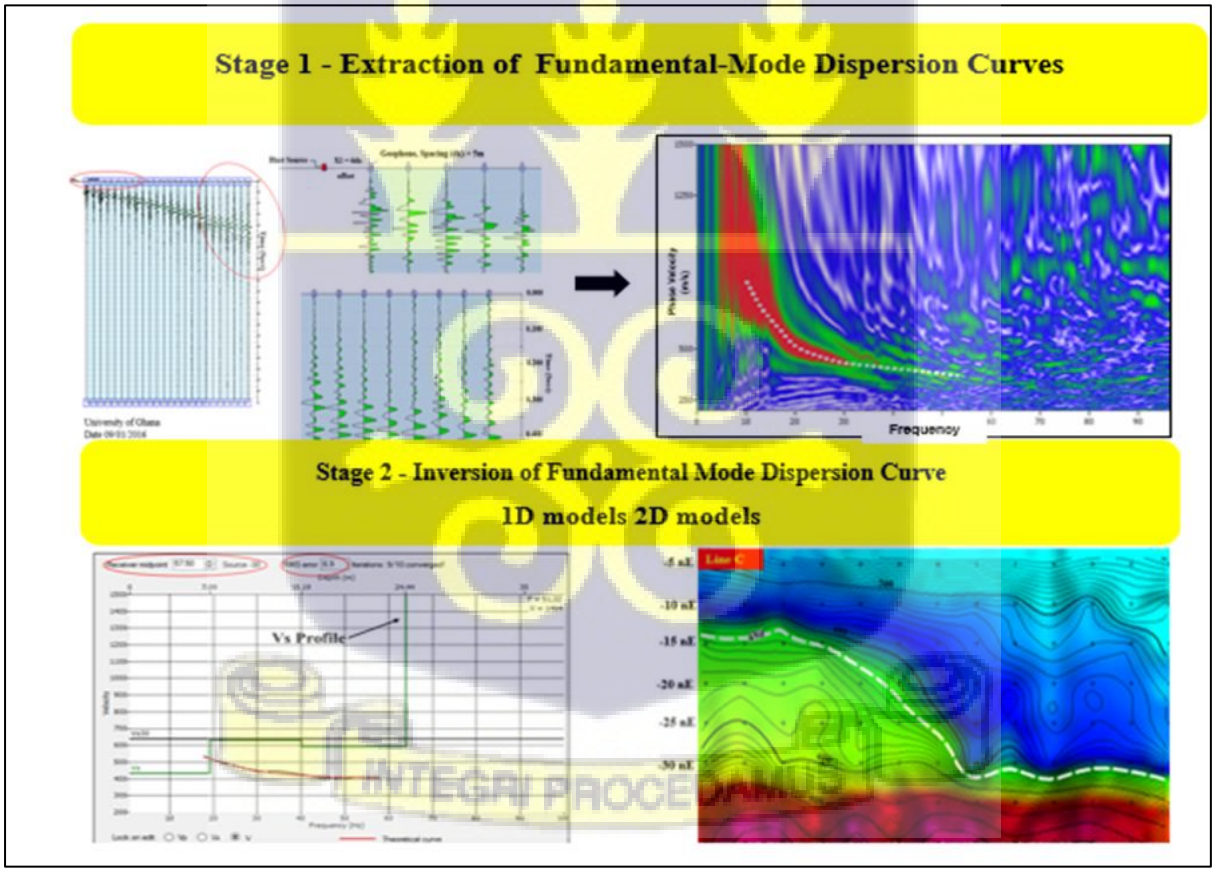

Figure 3.3 Generalized scheme for producing Vs profiles from MASW Data

Since the fundamental mode usually dominates the f –k spectrum (Tildy et al. 2003; Park et al. 2002: Stoke et al. 1994); i.e., showing with the highest energy among all wave packets, the seismic array (geophone spacing and the offset range) was optimized to obtain the accurate fundamental mode. This was subsequently used for all model inversions seen in the study.

During the inversion stage of data processing fundamental mode dispersion curves were automatically extracted by using an algorithm that follows the highest energy trends. These were then manually edited by discarding those outliers not fitting into a reasonable trend. Best fit curves for fundamental mode were extracted in the frequency range between ≈ 10 to 30 Hz.

Swept-frequency and the phase-shift methods (wave-field transformation method) are two common approaches used to extract dispersion curves from the recorded MASW data (McMechan & Yedlin, 1981; Park et al., 1998; 1999).

The Swept-frequency method is based on multichannel recordings that show trace-to-trace coherency in amplitude and arrival time of surface waves. The Rayleigh wave phase velocity at different frequencies may be measured by showing the multichannel record in a swept-frequency format. The phase velocities are calculated by computing the linear slope of each ground roll frequency component due to the linear separation of each frequency component (Park et al., 1999).

Noise sources (body waves and higher mode surface waves), are seen as gaps in otherwise coherent surface wave motion on swept-frequency records. Noisy data may be identified *in situ* with minimum effort since very little data processing is necessary to produce a swept-frequency record from an impulsive shot gather (no data processing is required if a vibrating seismic source is employed). Consequently, swept-frequency records allow for effective noise

reduction during data gathering by adjusting recording and/or field setup parameters, such as source-receiver offset (Park et al., 1999).

The phase-shift method (wavefield transformation method) is described by Park et al 1998, as a wave transformation technique to obtain a phase-velocity spectra (dispersion image) based on a multichannel impulsive shot gather. The method allows the dispersion properties of all types of waves (body and surface waves) in the recorded data to be shown in the frequency-phase velocity-transformed energy (summed wave amplitude) domain. Surface waves are classified into several modes based on their frequency content and phase velocity at each frequency. This efficient decomposition of the recorded data into different surface wave modes and various noise sources is a great advantage of the phase-shift method. Body waves and reflected or scattered waves, for example, are identified by their frequency content and moveout over the receiver array. For further analysis, the relevant Rayleigh wave dispersion curves are recovered from the dispersion image. In most cases, noise is reduced automatically throughout this procedure (Park et al., 2007). It also becomes possible with this technique to observe multi-modal surface wave dispersion characteristics, once the higher modes were excited during data acquisition (Park et al., 1998; Xia et al., 2003).

Figure 3.4 describes processing steps for the phase-shift method. A Fast Fourier Transformation (FFT) is applied to an n-channel impulsive shot gather ($u_j(t)$, j =1, 2,...,n), to decompose the record into individual frequency components ($\tilde{u}_j(\omega)$,j =1, 2,...,n). The amplitude of each trace of the record (in the frequency domain) is normalized to obtain $\tilde{u}_{j,norm}(\omega)$.

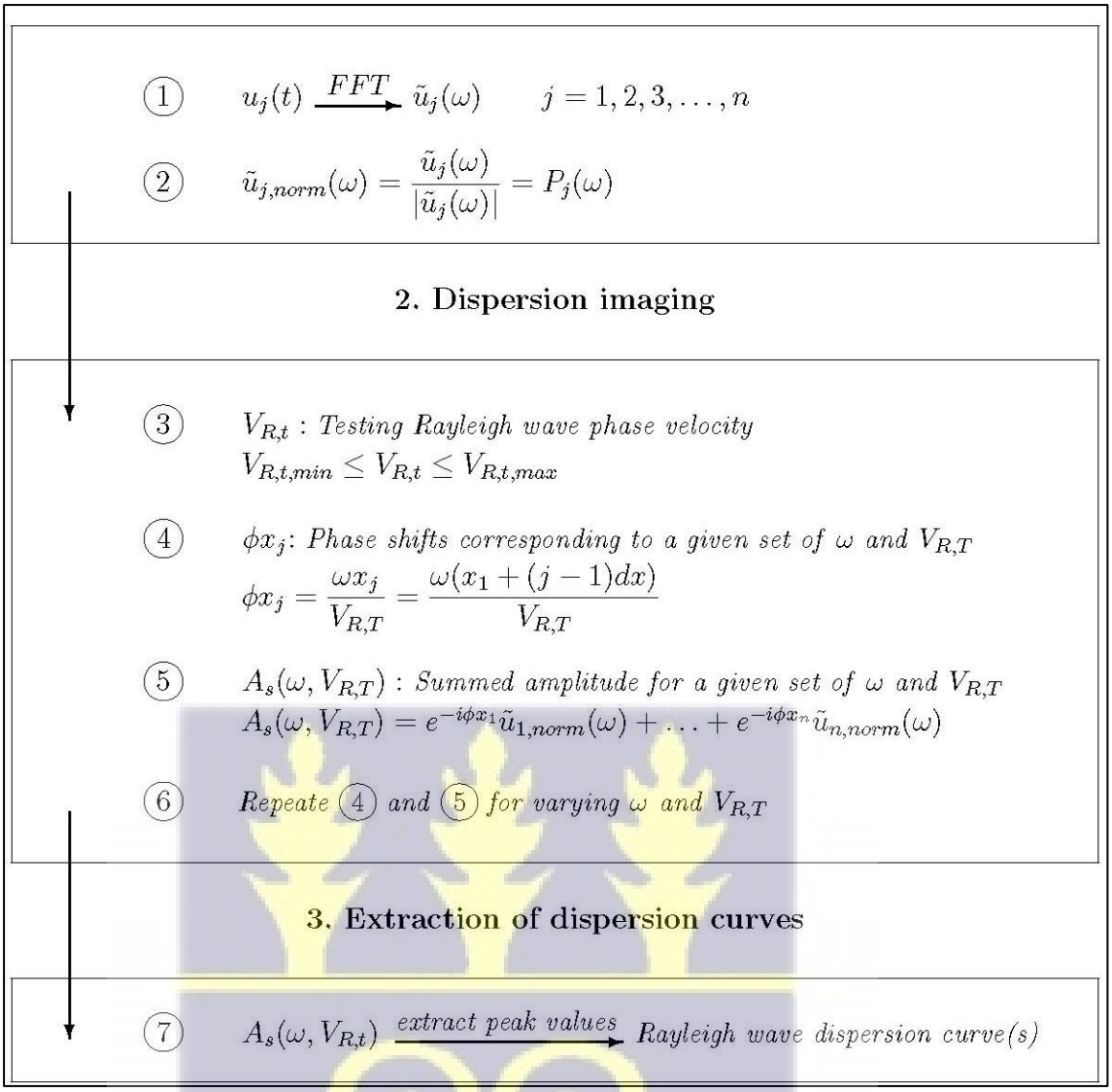

Figure 3.4 Overview of phase-shift method (after MASW, n.d.b; Park et al. 1998; Ryden et al., 2004)

As the phase spectrum of the signal ($P_j(\omega)$) contains all information about its dispersion properties, no significant information is lost. A phase velocity range for testing ($V_{R,T,min} \leq V_{R,T} \leq V_{R,T,max}$) is established. For a given testing phase velocity and a given frequency, the amount of phase shifts required to counterbalance the time delay corresponding to specific offsets are determined. The phase shifts are applied to distinct traces of the transformed shot gather that are thereafter added t to obtain the slant-stack (summed) amplitude corresponding to each set of ω and $V_{R,T}$. This is repeated for all the different frequency components of the transformed

shot gather in a scanning manner using varying test phase velocities, i.e. changing $V_{R,T}$ by small increments within the previously specified range. The phase velocity spectra (dispersion image) is obtained by plotting the summed amplitude in the frequency –phase velocity – transformed energy domain, either in two or three dimensions. The peak values (high-amplitude bands) observed display the dispersion characteristics of the recorded surface waves.

Easy MASW software was used for the interpretation and archiving of seismic data in the study. It is one of many easy-to-use applications for processing MASW data. Extraction of the dispersion curve is based on the phase shift approach. Data is imported from SEGY format and processing based on modes are displayed on a phase velocity – frequencies diagram of the dispersion of a user-defined stratigraphic model. Reports of velocity profiles is generated and geotechnical parameters, including average shear wave velocity up to 30 m, can be exported into *.DOC, *.DXF, *.BMP, *.JPG formats.

This relatively small number of iterations was chosen to minimize the effect of computational artefacts.

Sequential 1D Vs profiles compiled from inversion of the fundamental mode dispersion curves were stacked to generate 2D maps following schematic described above (Figure 3.3), and suggested shearwave velocity ranges by NEHRP or the IBC (BSSC 2001, IBC 2000) for 30 m depth of soil deposits.

3.2.1 Inversion and Model Parameters

Inversion of the extracted dispersion curves were performed using the algorithm by Xia et al. (1999). Calculations to derive shear wave velocity profiles, are based on wave propagation theory, assuming layered earth model (Figure 3.5).

Due to their non-linearity, inversion problems based on wave propagation theory are best solved using iterative approaches that compare previously obtained experimental curves with theoretical curve for a given model (Ryden et al., 2006).

The MASW method uses an inverse model to estimate a set of parameters that describe the soil deposit, based on an experimental dispersion curve. Dispersion for a layered earth model, depend on the number and thickness of soil layers and elastic properties of each layer. The elastic property of each layer is represented by, compressional wave velocity (Vp), shear wave velocity (Vs), and mass density (ρ). These physical properties are taken as constant and the last layer is assumed to be a half – space (Xia et al., 1990). Change in compressional wave velocity and density is insignificant so are often assumed (Tokimatsu, Member, Tamara and Kojima 1991). However, shear wave velocity has a dominant effect on the fundamental mode dispersion curve in a layered earth model, followed by layer thickness. One-dimensional (1D)

profiles are Vs profiles, with assumed no lateral variation for a given layered model. 1D profiles are the most representative of the subsurface materials below the receiver spread.

For the study, approximately four-varying-thickness layer model was created at the beginning of the inversion with the maximum depth (Zmax). Initial Vs model was created with the aid of phase velocity versus wavelength relationship depicted by the dispersion curve. Poisson's ratio of 0.3 and density of 2.0 g/cm^3 were assigned for all 4 layers during the inversion process. The iterative inversion was forced to stop after the 10th iteration of updating the Vs model.

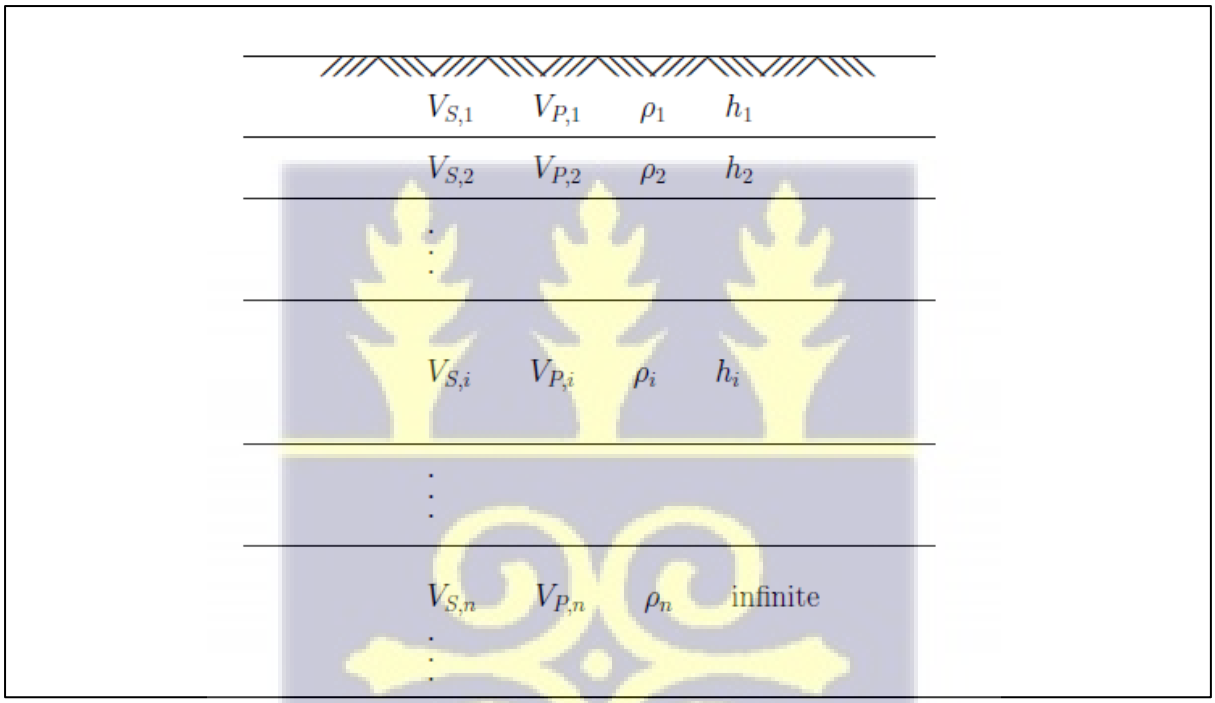

Figure 3.5 Layered earth model showing model parameters for inversion analysis. The last layer is assumed to be a half-space. (Vs – Shear wave velocity, Vp – body wave velocity, Mass density - ρ, and thickness – h).

3.2.2 Inversion Algorithms

Based on a set of input parameters, a mathematical model for layered elastic material is utilized to calculate a theoretical dispersion curve.

Matrix approaches based on wave propagation theory in layered material, are commonly used to determine theoretical dispersion curves. These approaches (e. g. Schwab and Knopoff 1970 and Kausel and Rosset 1980) are widely based on the Thomson-Haskell method.

The Schwab and Knopoff (1970) for example, has the benefit of enhanced computation speed and reduced overflow as well as loss-of-precision, resulting in higher accuracy (Schwab & Knopoff, 1970).

The Thomson-Haskell method, is a forward model based on the use of frequency-wavenumber domain transfer matrices (Haskell, 1953). It is also known as the transfer matrix method.

In an iterative process, various sets of parameters are added into the model in order to find the theoretical dispersion curve that best matches the observed dispersion characteristics.

The difference between the theoretical and experimental dispersion curves is frequently measured using the root-mean-square error between the two datasets**. (**MASW, n.d.d; Orozco, 2003; Xia et al., 1999). The accepted shear wave velocity profile can be identified as a one with the least difference between the experimental and theoretical dispersion curves.

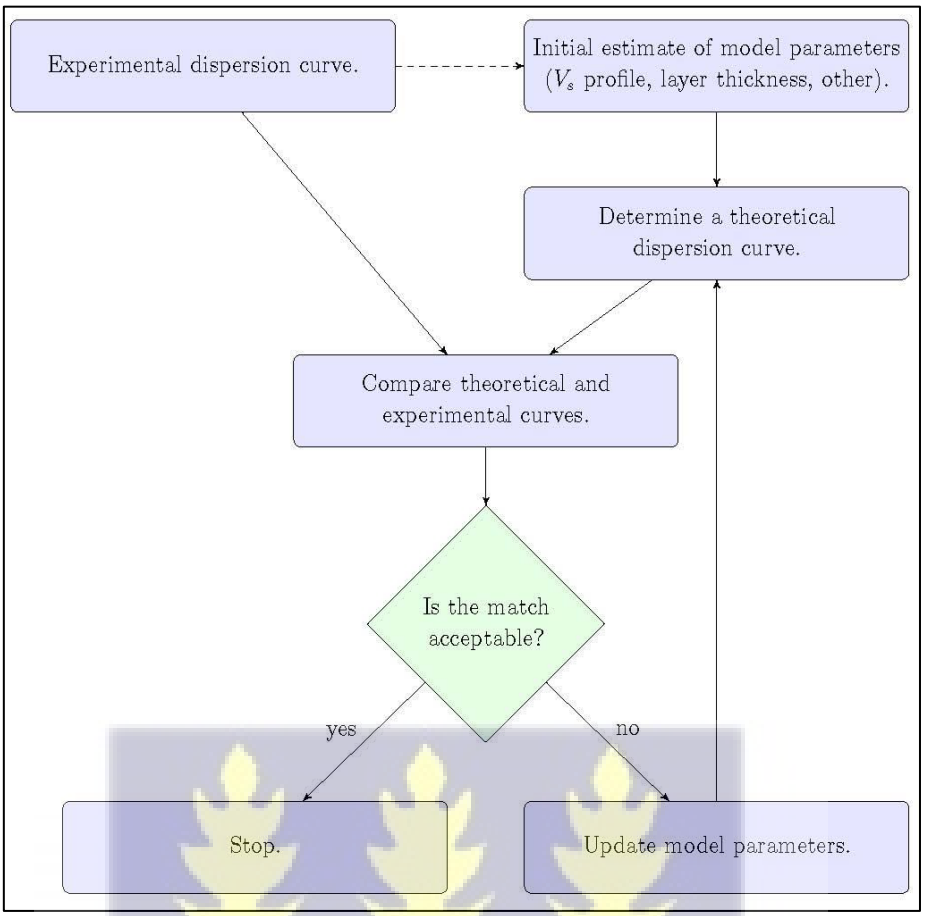

Figure 3.6 Overview of a typical local inversion algorithm

Based on how model parameters are updated between iterations during the search for the most probable set of parameters, inversion algorithms are divided into local or global search procedures (Orozco, 2003). Figure 3.6 is a schematic overview of a typical local inversion. Making an initial estimate of the needed model parameters is the first step in a standard local inversion procedure. Because the algorithm's convergence can only be ensured if the initial set of model parameters is sufficiently near to the final solution, a plausible starting guess is required. A theoretical dispersion curve is calculated based on the original estimate.

The problem is considered solved if the difference between the experimental and theoretical curves is acceptable. Otherwise, the set of model parameters is updated. A new theoretical dispersion curve is determined and compared to the experimental dispersion characteristics. The iterations continue until a reasonable match, in the vicinity of the initial estimate, is found or until the maximum number of iterations is obtained. If the curves do not converge, the initial set of model parameters must be changed. The experimental dispersion parameters are compared to a new theoretical dispersion curve. The iterations are repeated until a plausible match is identified as close as possible to the initial estimate, or until the maximum number of iterations is reached. The initial set of model parameters must be adjusted if the approach does not converge. (Orozco, 2003; Xia et al. 1999).

In global methods, the global minimum of the difference between a theoretical dispersion curve and the experimental data is sought by searching the whole solution space (Orozco, 2003).

A common method is to produce parametric sets at random within a predetermined range. Monte Carlo techniques are iterative approaches that use a random generator as well as iteration (Socco & Boiero, 2008). The survey's outcome is the set of parameters that provide the theoretical dispersion curve that best fits the experimental data.

Both local and global search strategies have their own set of benefits and drawbacks. Local approaches have a significant advantage over global methods in terms of processing speed. Local approaches, on the other hand, are often heavily skewed by the original prediction. When local search methods are used, the danger of finding a local minimum rather than the global minimum is high (MASW, n.d.d; Socco & Boiero, 2008). Easy MASW software used in the study, for data analysis is based on global search strategies.

CHAPTER FOUR

RESULTS AND DISCUSSION

4.1. Array Optimization and Data Quality

Shear wave velocity (SWV) data has been collected using Multichannel Analysis of Surface Waves (MASW) method, at forty-two (42) test sites within the GAMA.

Quality of data can be inferred from resolution of dispersion trend observed in the transformed wave field space (Park et al., 1998b). For the study optimal fundamental mode dispersion curve trends used for inversion, were obtained after test at various source-offset and spread-length configurations. Selected fundamental mode (10-30 Hz), dispersion curve, defined in phase velocity (m/sec) vs frequency (Hz) domain is extracted manually from each shot record along the trace in the image space. The fundamental mode is used because it shows with the most energy in the image space.

Results of three (3) field configurations, with different source offset distance and receiver spread lengths (D) is displayed in figure 4.1 below. These test configurations show the effect on horizontal resolution of dispersion curve development. For field configurations with the longest source offset distance (30m) and corresponding receiver spread length (90 m), dispersion curve resolution was very poor (Figure 41 d). Signal traces (Figure 4.1 a), show very low signal to noise ratio for datasets with this test configuration. Invariably, the resulting dispersion curve, in the image space, is dominated by higher-mode energy at the low frequency end of the phase velocity- frequency spectrum (seen as major velocity leakage at the beginning of the curve). Because the curve is largely influenced by higher order mode surface waves, the expected fundamental mode dispersion curve usually diverts from numerically expected

dispersion- curve trend (i.e., frequency values above 30 Hz). When inverted Vs over estimation will occur. This kind of data is rejected for the study.

Far field effects marked as incoherent signals toward the end of the signal trace (Figure 41 a), also occur when D is excessively long. Surface waves generated from this far offset shot point (-30 m) become attenuated below noise level at the far end of the receiver spread in the field geometry. Hence the signal becomes contaminated with high frequency (short wavelength) components of surface waves or body waves?

Moderate improvement in resolution and dispersion curve development is apparent in the image space, when receiver spread, length is reduced to 54 m, with an offset of 18 m (Figure 4.1b). Although resolution is relatively better here, there is still some velocity leakage at the beginning of the curve that may lead to slight overestimation when inverted. Further testing may be recommended to resolve depth resolution at such test sites. Optimal dispersion curve development resulted from test configuration with receiver spread length reduced of 36 m. Signal traces especially have highest signal to noise ratio (Figure 4.1 c) and best resolution for the dispersion curve (Figure 4.1 f) is seen. Here signal traces showed remarkably improved coherency (good signal to noise ratio). Velocity leakage is minimal and confidence in depth resolution for sample curves seen here, is high. Using this configuration, it is quite straightforward to recognize the different wave packets even from the signal traces (Figure 4.1c).

Also ensuring that the root percentage root mean square error (%RMS) of all the inverted shear wave velocity profiles used was kept below 5 % for each shot record analysed, guaranteed that, the shear wave velocity profiles derived from the inversion process are acceptable for developing the soil classification map of the study area.

The MASW technique here has successfully separated the surface waves from other noise. The resolution for the dispersion curve is consequently, excellent and even showed higher order mode Rayleigh waves (see end of image space, Figure 4.1 f).

It has become apparent that maintaining a relatively short receiver spread length for field configurations, MASW is effective in rejecting non-fundamental-mode Rayleigh waves and other coherent noise, resulting in optimized resolution of dispersion curve trends, for reliable results when inverted.

The compromise here is, though using larger spread length configurations results in poor horizontal dispersion curve resolution, more ground can potentially be covered, within the same space of time it takes to run surveys with shorter spread lengths. Hence reducing the number of roll-longs per line. However, with good resolution it is easy to identify fundamental mode in the image space, therefore helping to maintain a certain consistency in subjectivity throughout the entire dataset used for the study.

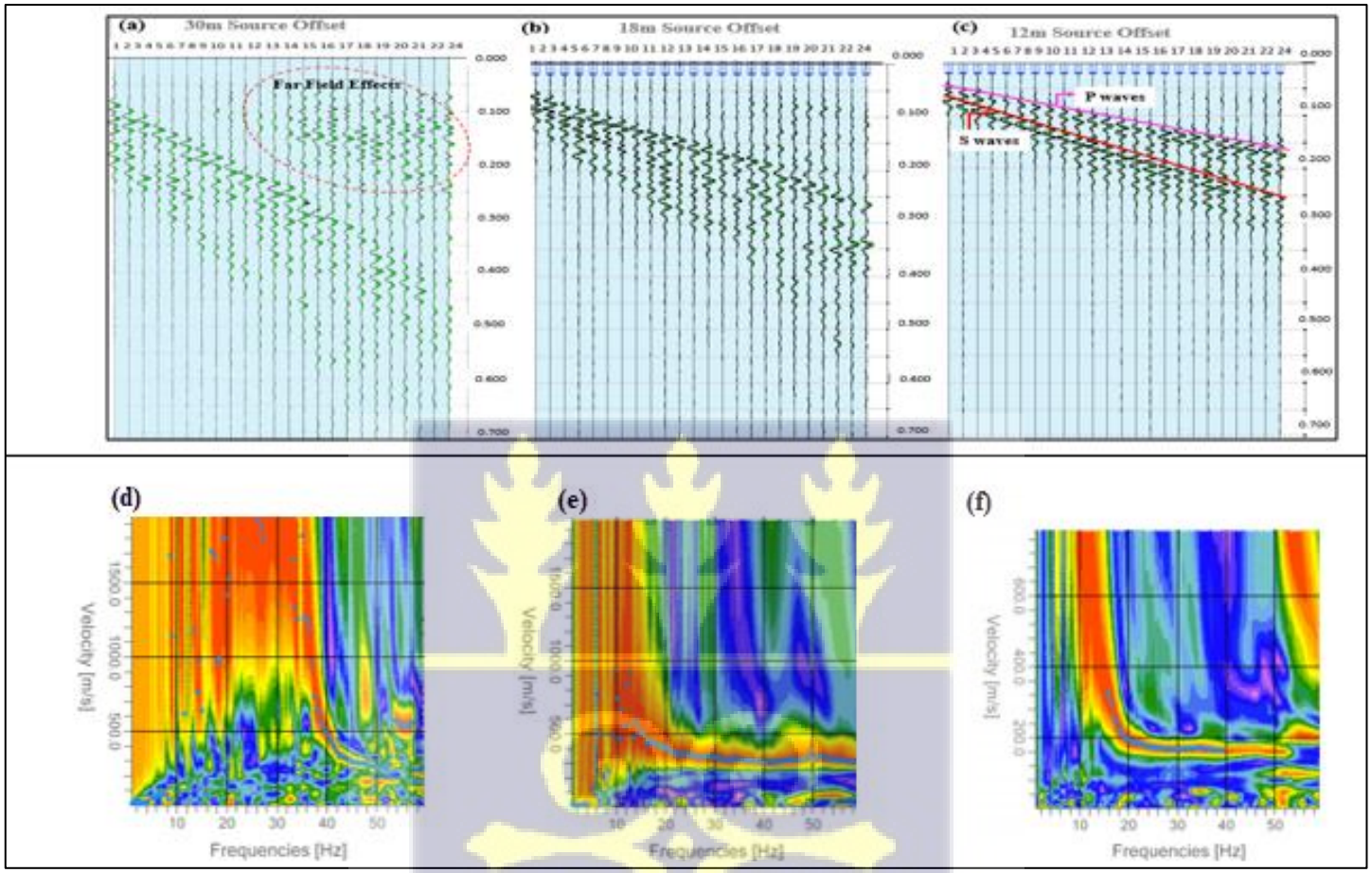

Figure 4.1 Effect of offset distance on dispersion curve development and data quality (a) raw surface-wave data acquired using, 4.5-Hz vertical-component geophones at 30m offset, contaminated by far field effects. (b) Improved coherency on signal traces at 18 m offset (c) Effect of decreased offset distance on signal traces at 12m offset. Traces show good signal to noise ratio. (d) Data image from 30 m offset in phase velocity – frequency domain. (e) Data image from 18 m offset in phase velocity – frequency domain. (f) Data image from 12 m offset in phase velocity – frequency domain (Fundamental mode at end of image space).

To investigate drastic or otherwise, any anisotropy in the data collected, mean shear wave velocity is calculated for data in two (2) primary orientations; approximately, north-south and east-west.

From summary statistics below, mean shear wave velocity (SWV) calculated for data in both orientations, only show marginal differences. Mean SWV for lines oriented in the NE-SW direction is approximately 505.26 m/s, while SWV in the opposite direction increased marginally to approximately 508 m/s). Both values registered moderate shear wave velocity for 30 m of soil; a transition between soft soils and bedrock type velocities (NEHRP 2003, NEHRP 2009).

Table 2 Summary Statistics – Anisotropy Tests

Summary Stats Lines NE- SW		*Summary Stats Lines NW-SE*	
Mean	505.56	Mean	507.94
Standard Error	32.32	Standard Error	33.61
Median	476.45	Median	457.38
Mode	#N/A	Mode	#N/A
Standard Deviation	171.04	Standard Deviation	181.04
Sample Variance	29255.92	Sample Variance	32774.65
Kurtosis	-1.048	Kurtosis	-0.178
Skewness	0.40	Skewness	0.79
Range	562.17	Range	635.32
Minimum	258.36	Minimum	272.7
Maximum	820.53	Maximum	908.02
Sum	14155.73	Sum	14730.38
Count	28	Count	28

4.2. Site Characterization and Soil Classification for the GAMA

Shear wave velocity (SWV) in the shallow subsurface is important for comprehensive determination of dynamic behaviour of soil.

Vs30 is particularly important in earthquake engineering design. Many building codes; Uniform Building Code (UBC) and Eurocode 8 (EC8) codes etc., use Vs30 to classify sites according to the soil type.

Based on the direct measurement of shear wave velocity and suggested seismic site classification scheme according to the National Earthquake Hazard Risk Program (NEHRP) for the top 30 m depth of soil deposits (Vs30), a new soil classification map for a major part of the GAMA is suggested.

Shear wave velocity profiles of the tested sites were obtained by inverting the dispersion data of the fundamental mode Rayleigh waves. Derived Vs30 is correlated to descriptive characteristics described in table 3. These are applicable standard classifications similar to those found in UBC and EC8 and other well-known building codes around the world.

From direct measurement of SWV at 42 locations (Figure 4.2) within a major seismic region of the GAMA, an extensive database of calculated near-surface shear wave velocity, is compiled for comprehensive assessment of soil conditions and seismic site effects within the GAMA.

In Ghana this area bears significant importance to seismic safety. Many authors; Amponsah et al 2008, 2012, Ayetey and Andoh 1998, have highlighted how the large convergence of dynamic features (major historical earthquakes, major and minor active faults, many recent impactful tremors) within this densely populated and haphazardly planned region, constantly exposes the region to the affiliated disasters of earthquakes on a daily basis (Figure 4.3, Figure

4.4). Some important infrastructure such as the Weija dam, West hills mall and several beach resorts are also sited here.

Table 3 Site classification scheme according to recommended scheme by the NEHRP (NEHRP 2003, 2009)

Soil Profile	Vs30 Value (m/s)	Soil Description	Value Breaks
A	> 1500	Hard Rock	
B	760-1500	Rock	
C	360-760	Dense Soil	
D	180 - 360	Stiff Soil	
E	< 180	Soft Soil	
F		Special Soils requiring special evaluation	

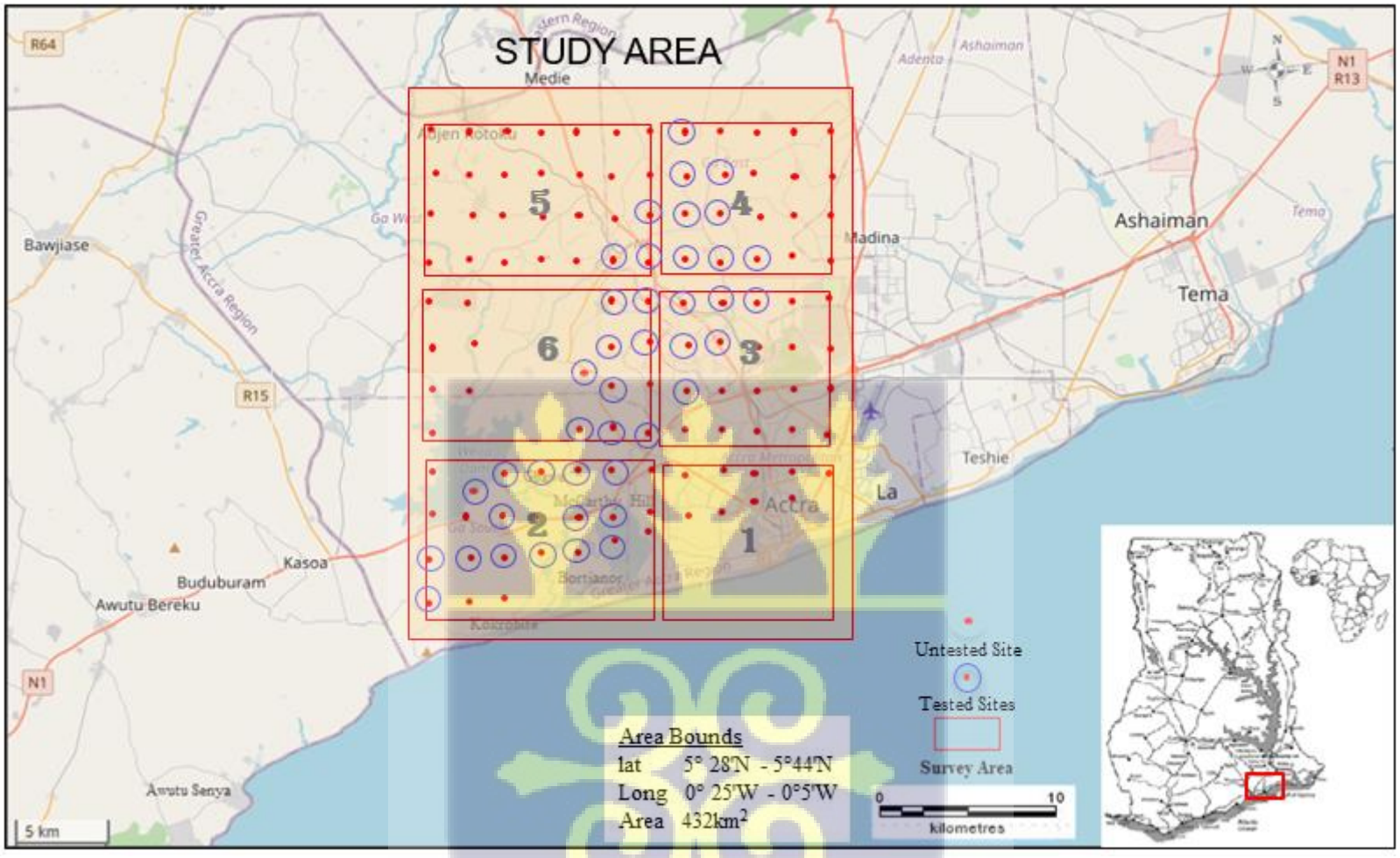

Figure 4.2 Location Map of the GAMA (study area highligthed by shaded space)

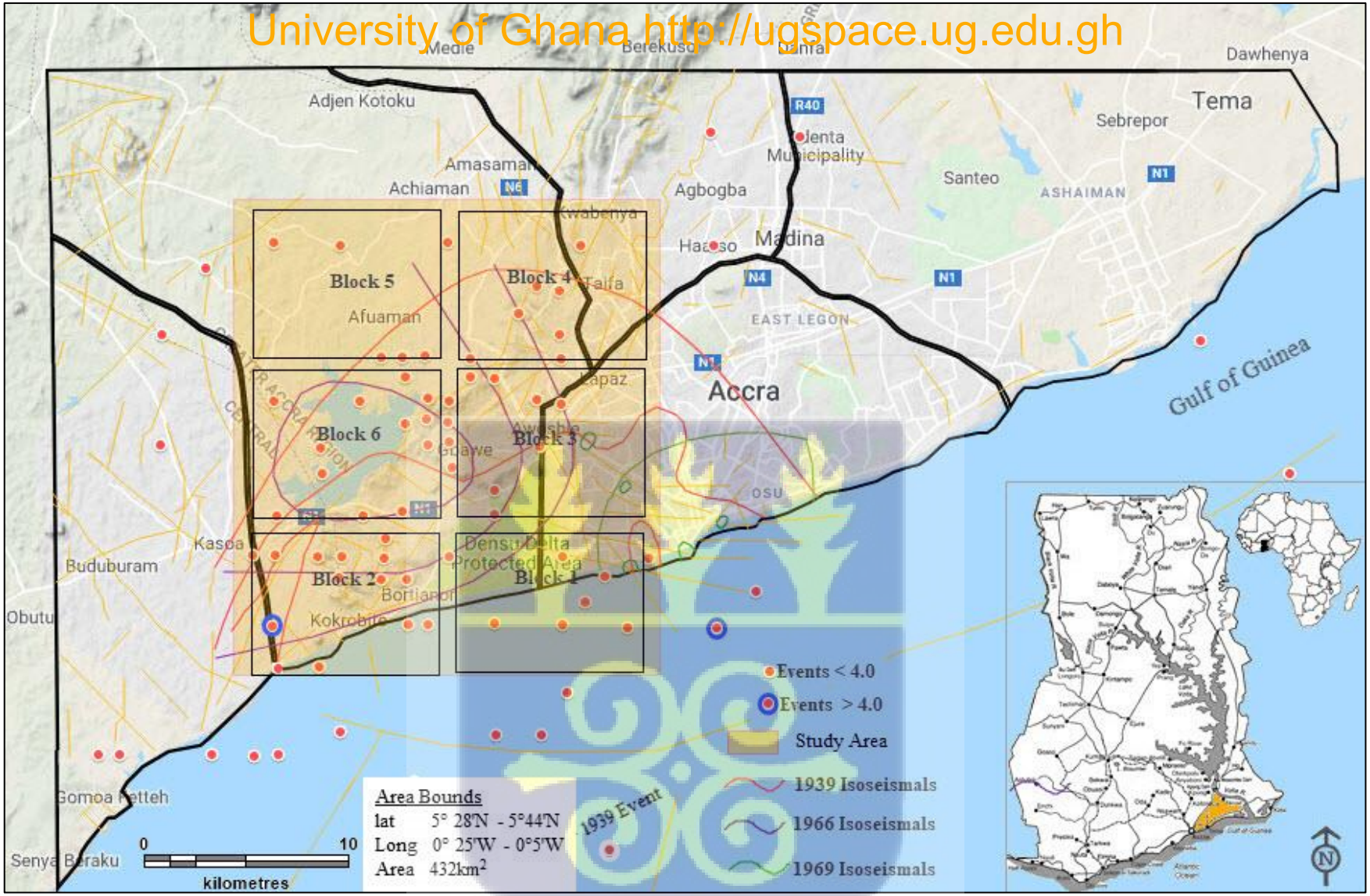

Figure 4.3 Map of the GAMA Showing large convergence of dynamic factors (Faults, isoseosmals, historical and recent events)

Figure 4.4 Images Showing lapses in built environment in study area

(Curtesy Joy FM, https://www.publicagendagh.com/the-looming-weija-kasoa-ridge-disaster/05.09.2021)

4.2.1 Shear Wave Velocity Distribution for the GAMA

Distribution of mean shear wave velocity with depth is calculated for the study area. Table 4 shows summary statistics of calculated mean shear wave velocity for four (4) different depths; 5 m, 15 m, 30 m and 40 m. These were calculated in order to assess variation of SWV with depth over the study area, and also the influence of topography, if any, on shear wave velocity distribution. Topography within the work area increases generally from the south towards the north (Figure 4.5, test sites used in the study are marked as white dots on SRTM). The lowest elevations are mostly found within the area marked block 2.

Average shear wave velocity for the depth ''d'' of the soil referred as V_{Sd} is computed as follows:

$$V_{Sd} = \frac{\sum d_i}{\sum(^{d_i}/_{v_i})} \quad \text{.....Eq. (8)}$$

where: d = $\sum d_i$ = cumulative depth in m. Therefore for the top 30 m depth, the shear wave velocity was estimated as:

$$V_{S30} = \frac{30}{\sum(^{d_i}/_{v_i})} \quad \text{..... Eq. (9)}$$

where: d_i and v_i denote the thickness (in meters) and the shear wave velocity in m/s of the i^{th} layer in a total of N layers, existing in the top 30 m.

Table 4 Summary Statistics – Mean Shear Wave Velocity with Depth

	Vs5	*Vs15*	*Vs30*	*Vs40*
Mean	**185.4893**	**259.9105**	**497.6019**	**548.823**
Standard Error	8.2338851	10.669826	27.250432	32.599182
Median	188.6758	259.52	457.185	507.06
Mode	#N/A	#N/A	#N/A	#N/A
Standard Deviation	49.4033110 6	64.0189563 7	163.502595 3	192.859366 2
Sample Variance	2440.68714 4	4098.42677 5	26733.0986 8	37194.7351 5
Kurtosis	-0.90159	-0.50012	-0.42452	-0.2360
Skewness	-0.1382	0.106908	0.664450	0.75570
Range	172.92	254.96	569.62	685.39
Minimum	**95.85**	**137.26**	**268.43**	**297.52**
Maximum	**268.77**	**392.22**	**838.05**	**982.91**
Sum	6677.615	9356.779	17913.67	19208.8
Count	36	36	36	36

Distribuition of shear wave velocity for the first 5m (Vs5) of soil, does not vary significantly in range over the entire area (Figure 4.6 a). The highest values (deeper shade of blue) within the range are aparent toward the northern part of the study area. Topography here is generally higer here, than in areas to the south, for instance, block 2. Calculated values vary within a relatively narrow range of 95 m/s and 268 m/s (Figure 4.6 b). Overall Vs5 for the entire area points to wide spread deposits of loose to medium cohesionless soil or predominantly soft to sligltly stiff cohesive soil for the first 5 m of soil (see Table 3).

Moving downwards, to 15 m (Figure 4.6 a), shear wave velocity also shows no drastic lateral change in range of values. Shear wave velocity for 15 m (Vs15) of depth is between 137 m/s to 392 m/s, with a mean of 259 m/s. This suggests that, below 5 m, soils are characterized by slightly stiff soils.

Moderate (360 -760 m/s) velocities are found at depth north of block 2. The anomaly (green colour) only becomes apparent after calculating Vs30 and Vs40 (Figure 4.6 a). Here elevations are generally higher, compared to the areas in and around block 2. The value range of Vs30 and Vs40 (see mean, table 4), suggest predominantly dense soils at significant depth (below 15 m).

Figure 4.7 shows two (2) sample velocity-depth profiles within block 2, where elevation is lowest within the study area (Figure 4.5b). These profiles show significant velocity inversions in a two-layer model, possibly from some fracturing. Bedrock type velocities are not apparent here, until ≈25 m and below, where moderate velocities affiliated with dense soils are present at depth. In figure 4.7 b, low velocities are found at depth, suggesting soils may not be prevalently densely compacted throughout the entire profile. 2D depth profiles (Figure 4.7 c and d) show predominantly with SWV values within a range of 180-360 m/s. These values are very low, indicating that the soils may be significantly vulnerable to ground motion, especially within southern part of block 2.

At higher elevations sample profiles (e.g., near block 3), bedrock type velocities are apparent at approximately, 15 m depth (Figure 4.8), within a dense matrix of competent weathered rock (Figure 4.8 b). The 1D profile shows a classic 2-layer depth model, characterized by increasing velocity with depth.

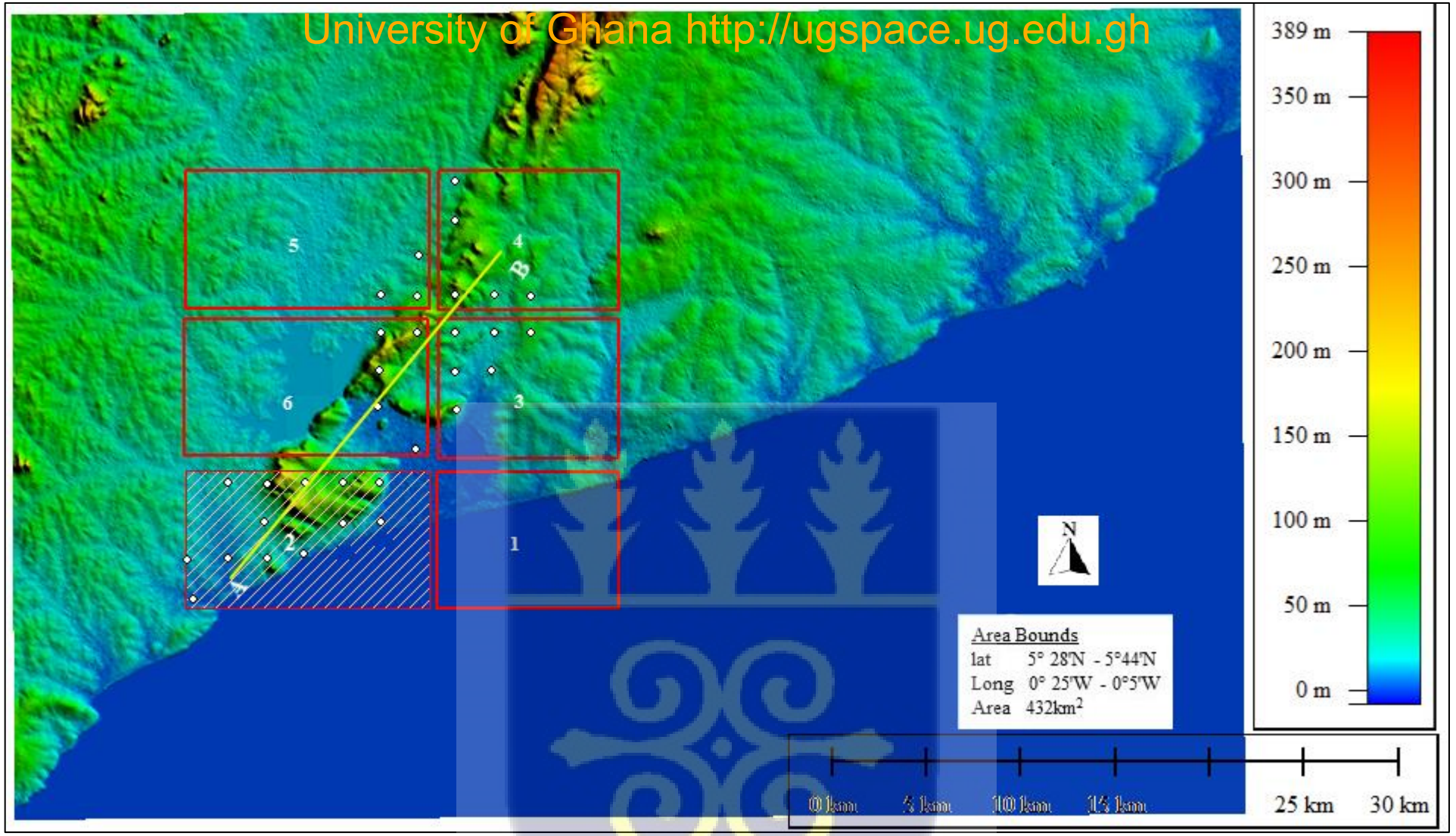

Figure 4.5a SRTM for the GAMA

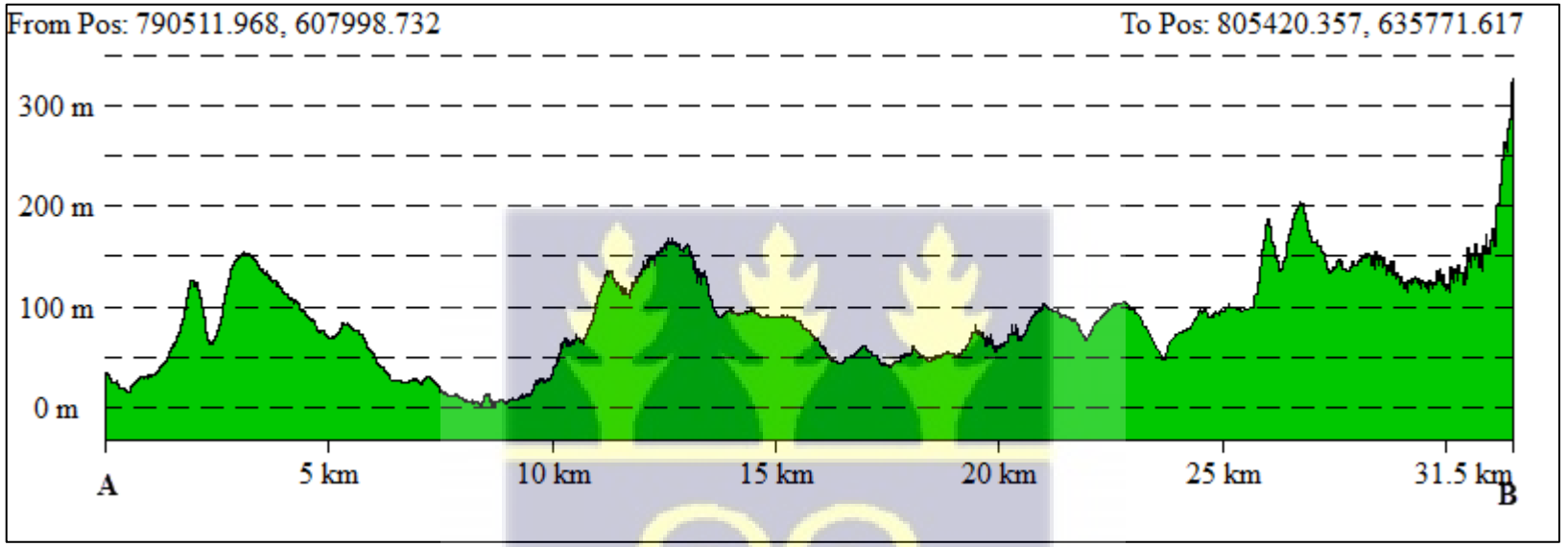

Figure 4.5b Horizontal Elevation Path Profile from block 2 to Block 4

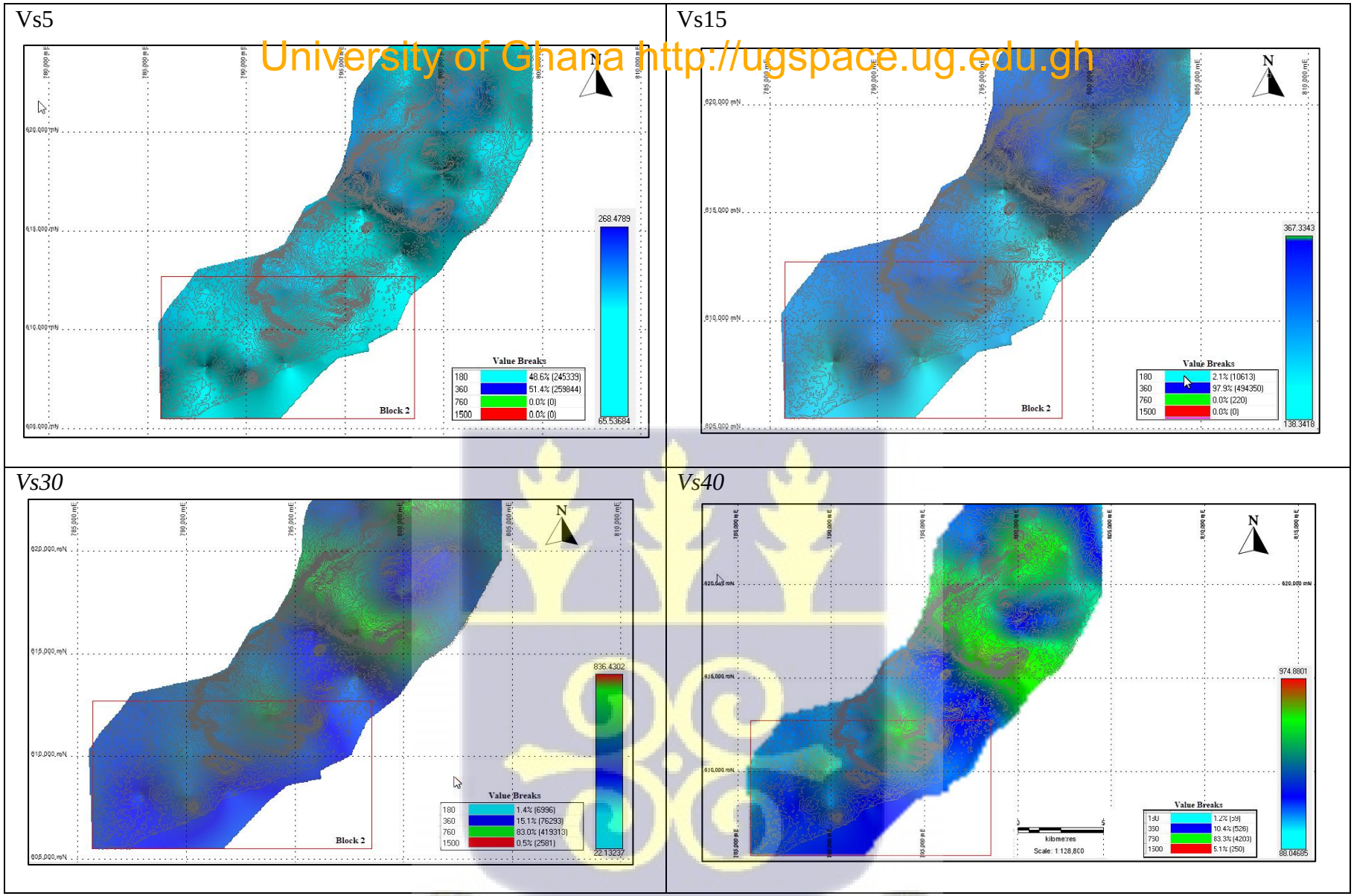

Figure 4.6a Figure 4.6a Average shear wave velocity distribution maps of the GAMA down to 5 (Vs5), 15 (Vs15), 30 (Vs30), and 40 (Vs40) meters depth

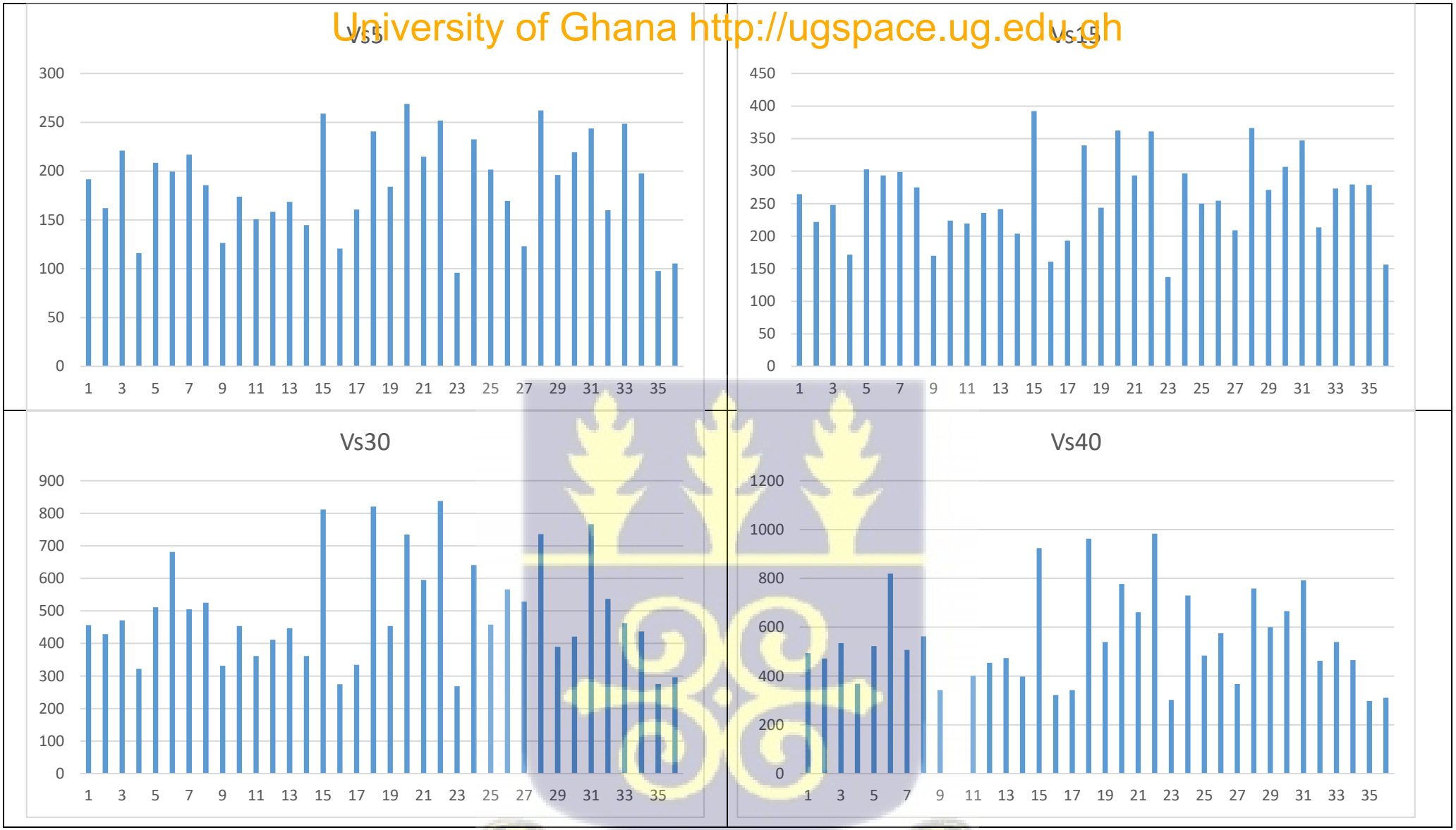

Figure 4.6b Histogram of Vs5, Vs15, Vs30 Vs40 values

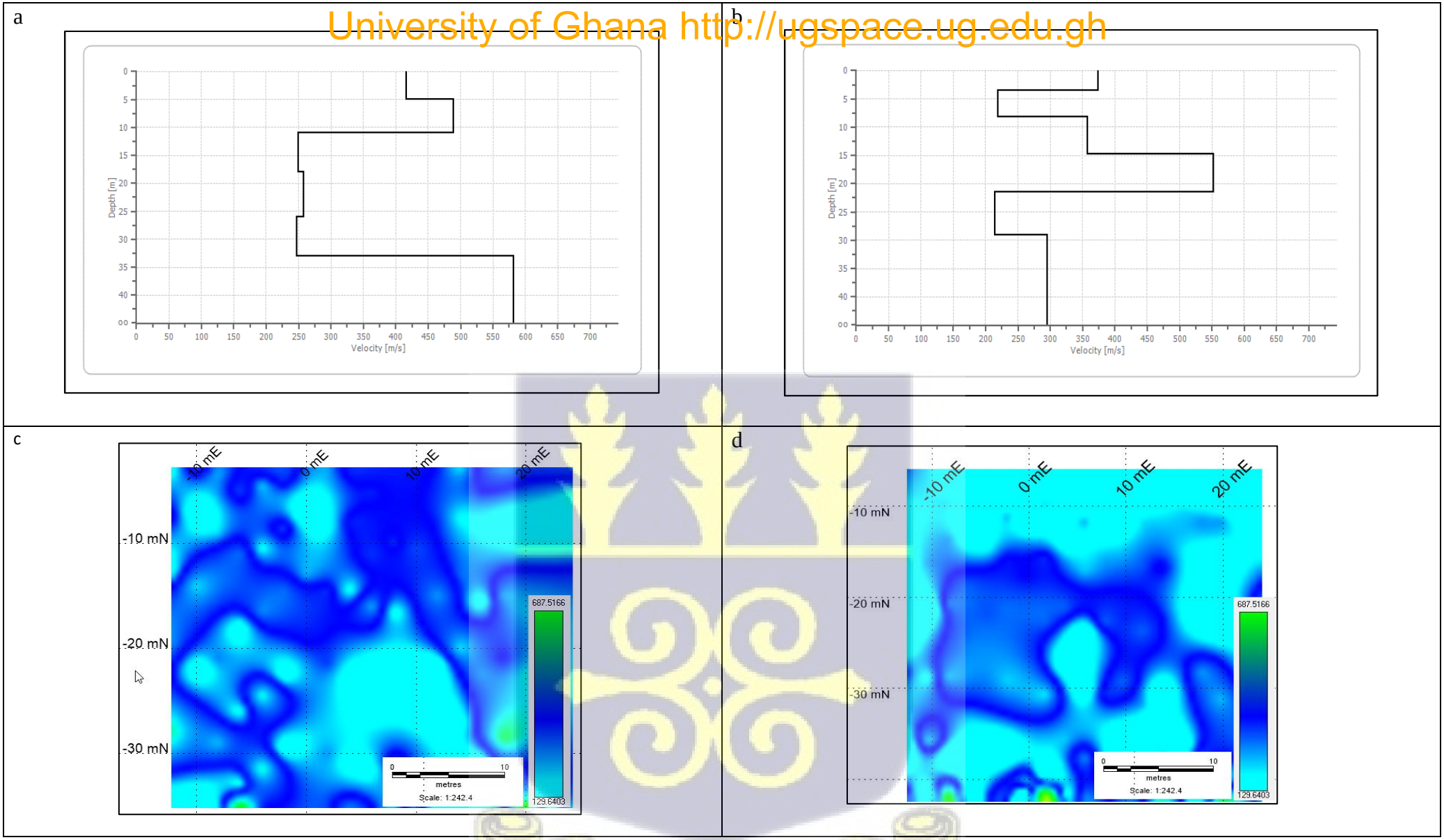

Figure 4.7 Depth Profiles within Block 2

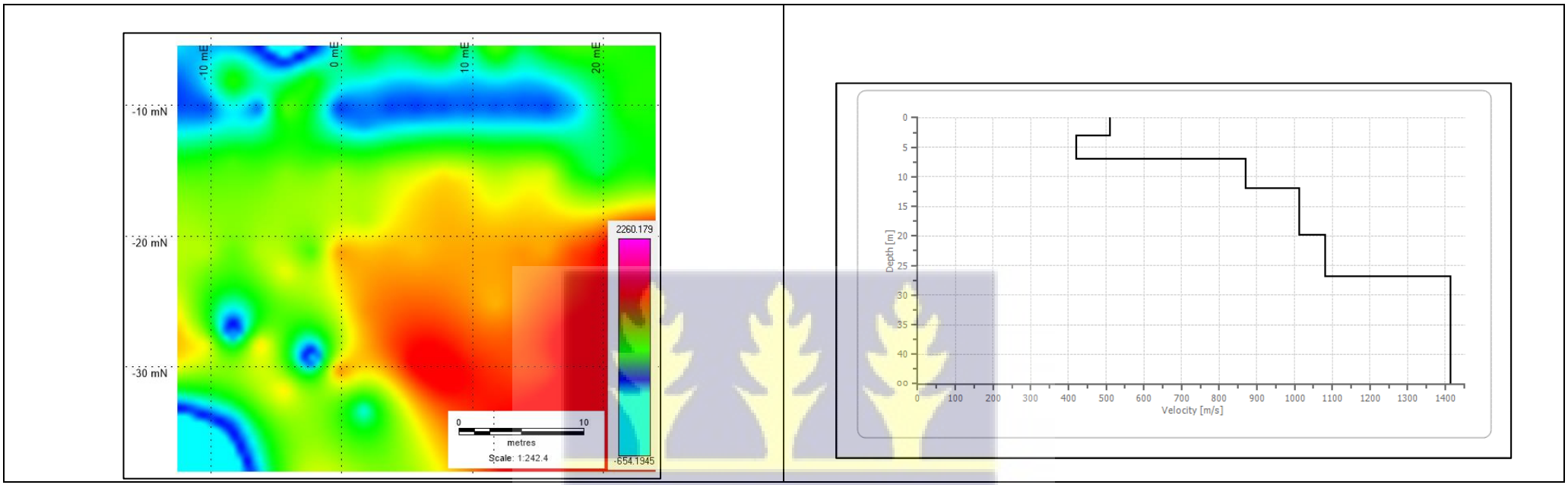

Figure 4.8 Depth Profiles at Higher Elevations near block 3

4.2.2 Local Soil Conditions and Site Classification for the GAMA

Seismic site effects based on SWV is one of the important direct indicators of damage distribution. Local site effects refer to the seismic ground response characteristics of individual soil sites, and it is common to find this incorporated into most modern seismic design code provisions in many countries. Ground motion is influenced by the geotechnical features of soil deposits, and modifications to ground motion is due in part to shear stiffness. Site classes correlated to SWV of the soil column, are found in most design code and are defined in terms of SWV up to a depth of 30 m (Vs30). If measurement of SWV up to 30 m is not feasible, SPT-N or undrained shear strength (Su) can be used (Borcherdt 1994). Effective damage distribution assessment requires strong recorded ground motion amplitudes and local site parameters (Roca el al., 2006).

A complete catalogue of earthquake ground motion has been compiled for the GAMA (Amponsah et al 2012). Extensive regional seismic site effect studies for improved seismic hazard assessments, is yet to be completed for the GAMA.

Central to the study is site response and classification for the area. Although many areas still remain untested (Figure 4.2), for the present study a major part of the GAMA has been investigated and classified according to NEHRP site classification scheme for 30 m of soil (Figure 4.9).

From measurement of SWV up to depth of 30 m, two main site classes (C and D) have become apparent.

Mean shear wave velocity up to 30 m, for the study area is approximately 500m/s (Table 4).

Figure 4.9 shows that generally, Vs30 for the south of the study area (Block 2) is within a range of 180 -360 m/s. Moderate velocities show toward the some parts of the central and the north of Block 2. This is seen clearer when looking northeast – southwest (Figure 4.10).

From calculated SWV, a large part of the GAMA belongs to designated site class D (Figure 4.9). Overlaying Vs30 map over the geology of the GAMA two (2) subdivisions for site class D (D1 and D2) is suggested.

Designated site class D1 is identified at two (2) main areas within the study area; south and northwest of the study area. The areas to the south, mainly within Block 2 are predominantly classified as site class D1.

D1 southwest of the study area is a very important site. This block includes Tuba, Bortianor, Bojo, Korobite and Nyanyano, which is close to the epicentre of the last major earthquake in Ghana (See table 1).

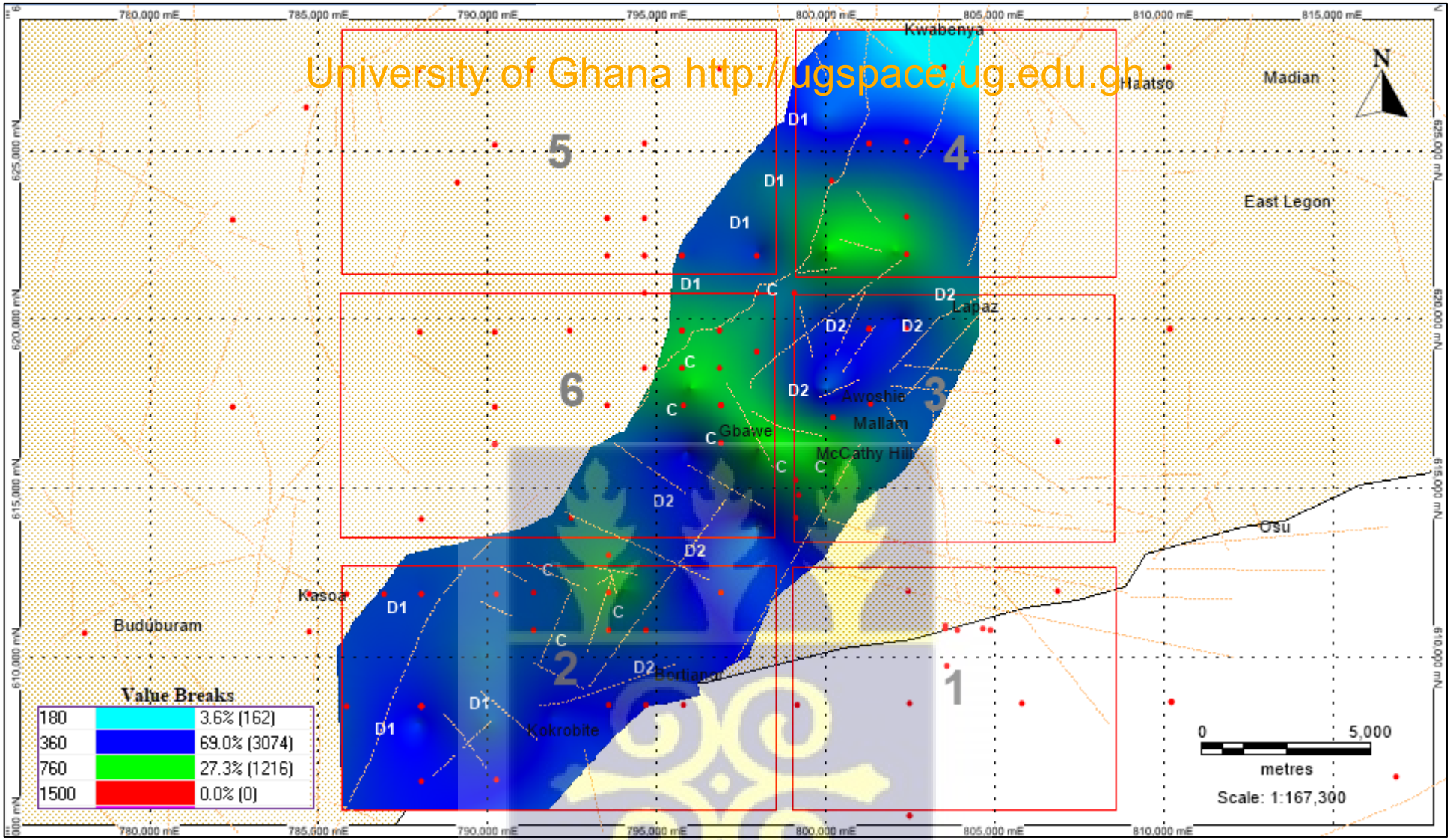

Figure 4.9 Soil classification map of a major part of the GAMA according to the NEHRP site classification scheme for 30 m of soil.

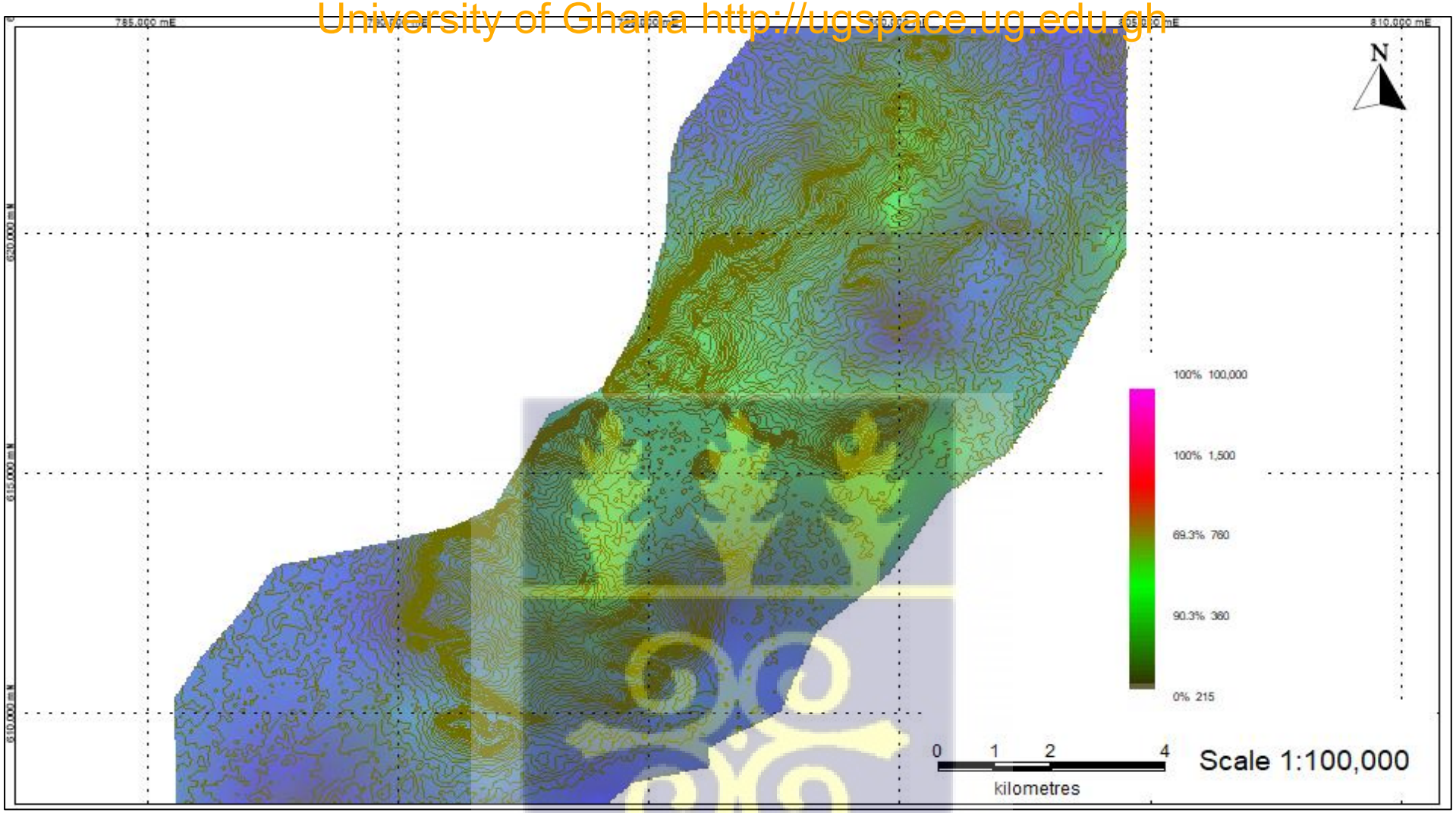

Figure 4.10 Vs30 looking NE – SW

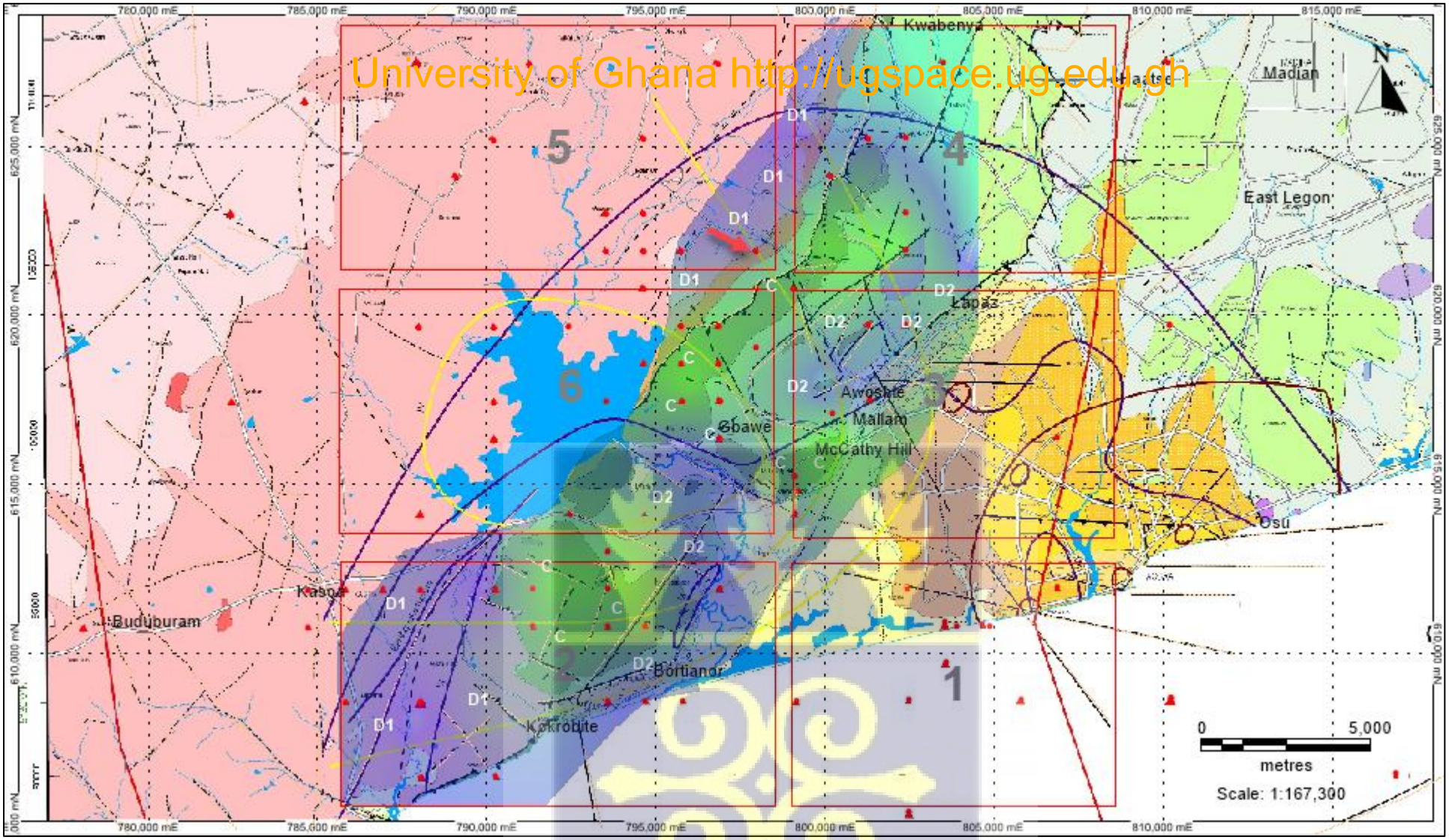

Figure 4.11 Vs30 Overlaid Over Geology of GAMA (Vs30 40% Transparent)

D1 within block 2, and D1 north of the study area (Figure 4.10) are both underlain by residual soils of granitoids of the Birimian; migmatitic biotite hornblende granitoids, deeply weathered granitoid-pegmatite complex and porphyritic granites (see summarized geological map legend, figure 1.6). The Vs30 values here range between 180 and 360 m/s. These values are at the lower end of the NEHRP site classification scheme and, commonly characterize stiff soils. Soils with lower shear wave velocity values (below site class A and especially within site class E or F) will experience more ground motion than those that show with bedrock type velocities (e.g., site class A).

Although seismic site response for residual soils assigned class D2 are similar in range to the D1 discussed above, Residual soils that characterize dispersion spectra for D2 are derived from the phylite units in the GAMA. This unit is mapped as often talcy, with interlayers of thin quartzitic bands, chert, or quartz-schist. D2 covers the middle and to the northeast of the study area.

Four important depth profiles are shown in Figure 4.12. These are results from D1 north (Figure 4.12 a and b) and D1 south (Figure 4.12 c). All profiles do not show with bedrock type velocities.

Generally, the profiles are characterized by very low SWV even after 30 m depth. Both sample test sites are underlain by GAMA granitoids.

Figure 4.12 d shows a very unique depth profile for site class D1. The location for this (small red arrow in figure 4.11) depth profile is near the lithological boundary between the GAMA granitoids and the phyllite (Phyllonitic units) of the Togo to the northwest of the study area.

The depth profile shows low SWV (180-360 m/s), characteristic of the granitoids, which grades sharply to moderate type SWV values (360 – 760m/s), marking a suggested lithological change between the two units.

Similar to D1, depth profiles for D2 are also very low SWV values (Figure 4.13). Bedrock type velocities are not seen here.

In general, these profiles (Figure 4.12) show significant amount of very low SWV (sometimes less than 180 m/s) at significant depths within stiff soil. This indicates that soil profiles are not uniformly compacted within this area. These soils are significantly vulnerable to ground motion.

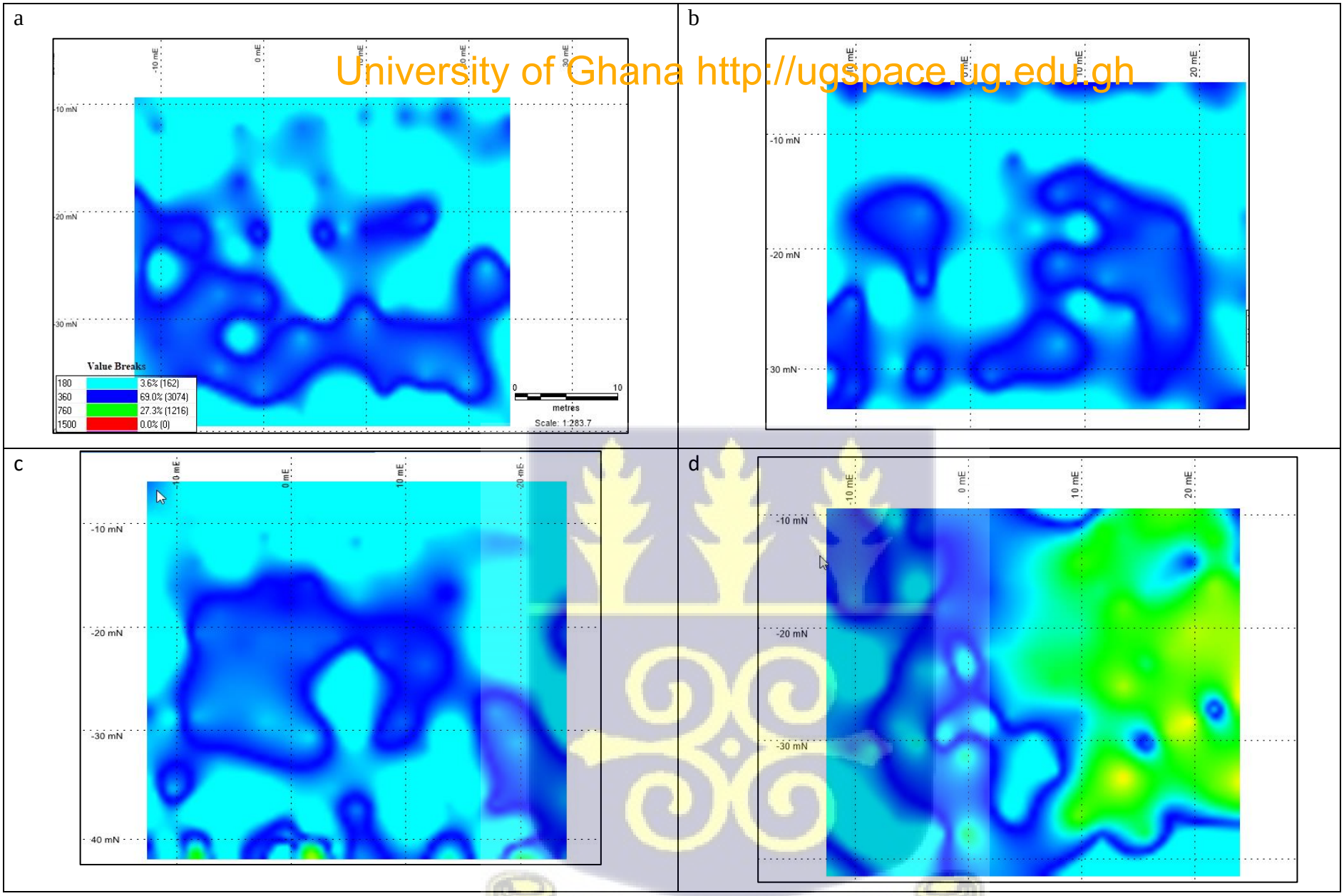

Figure 4.12 Vertical Profiles D1 North and South of Study Area

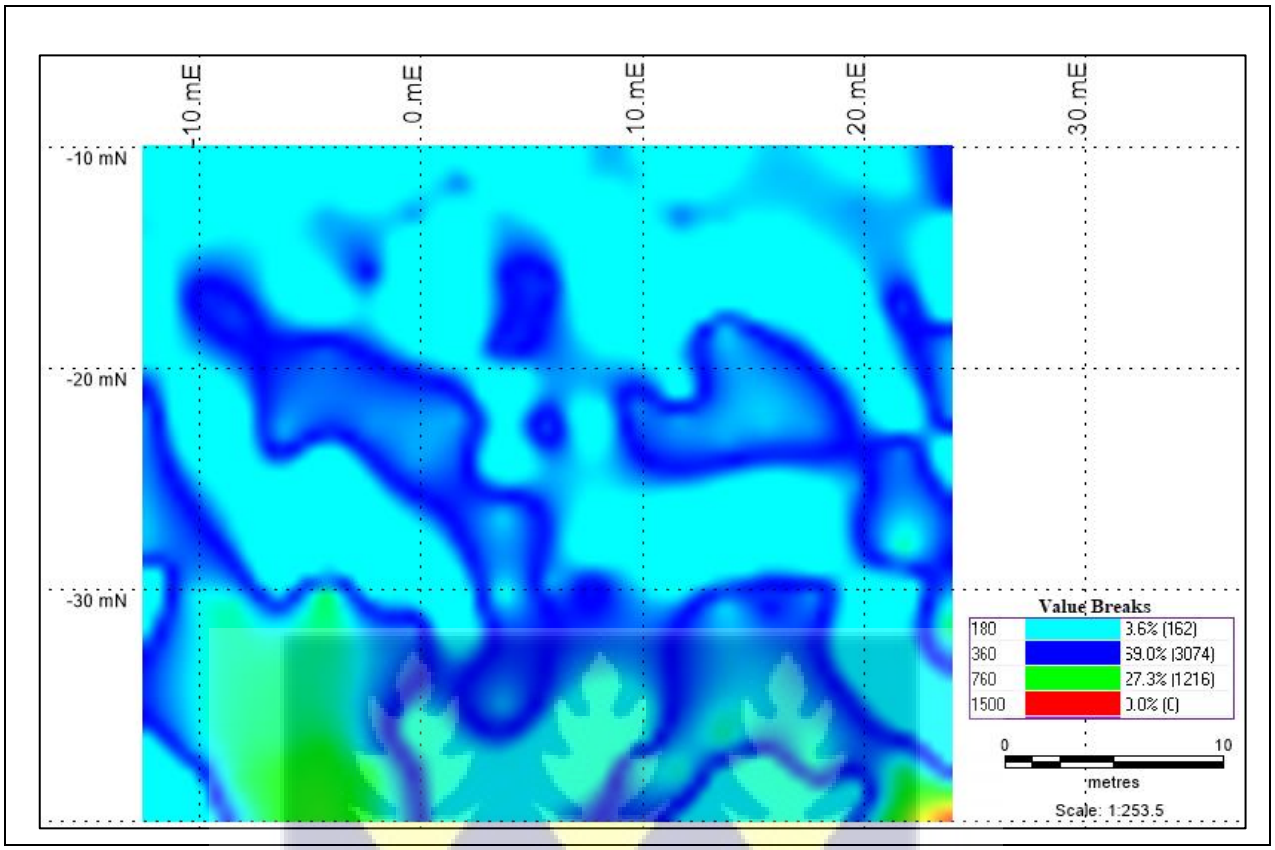

Figure 4.13 Depth Profile for D2

a

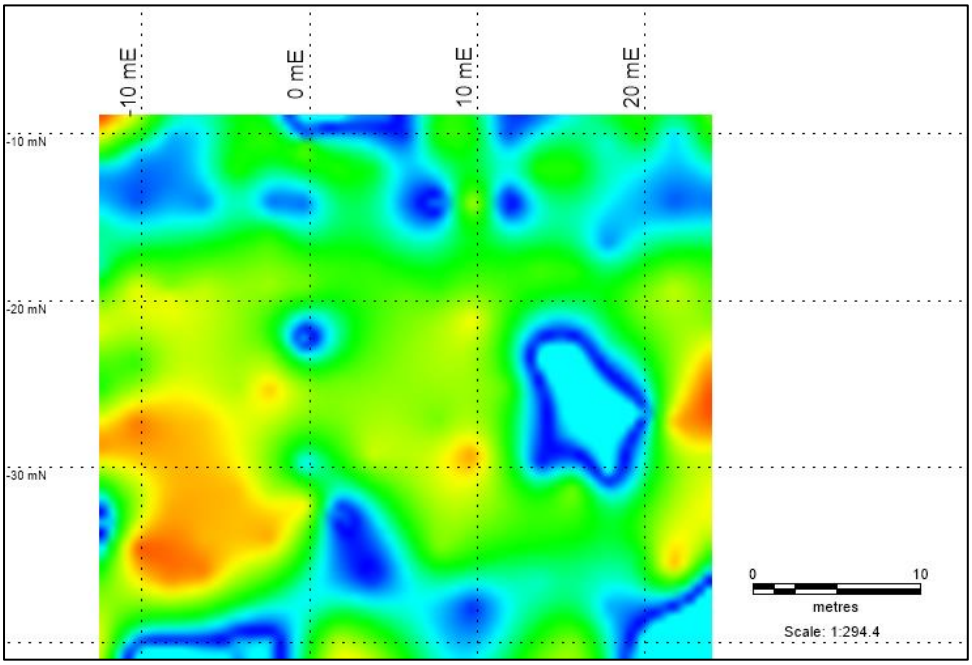

b

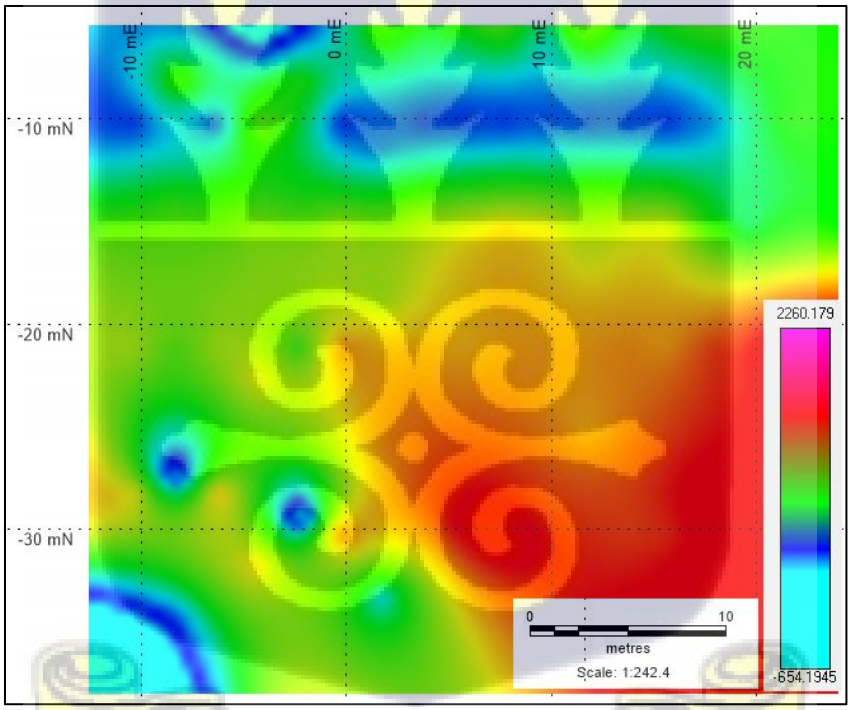

Figure 4.14 Depth Profiles for site Class C

Moderate to more competent soils (site class C) is found to the south (top part of block 2) and north mainly between block 6 and 3. In these areas, Vs30 is within a range of 450 m/s to 760 m/s. Residuals soils here are predominantly from quartz-schist and quartzite units (sericitic quartz schist, with interlayers of quartzitic bands, phyllite or chloritic schist or phylite.

The depth profiles here (Figure 4.14) have moderate SWV values, usually with deep soil profiles of dense weathered soils and bedrock type velocities are commonly encountered at depth (≈15 m).

In general soil profiles for site class D, are characteristically deep, with low SWV and major velocity inversions at depth, suggesting lack of considerable uniform compaction and several dynamic features (e.g., faults, fractures, voids etc.,) that make these soils relatively more vulnerable compared to soils classified as site class C. Bedrock type velocities are rarely encountered at depth. Depth profiles for site class C on the other hand have moderate SWV and bedrock is commonly found at depth (after 15 m). These are shallow soil profiles and more competent sites, especially at higher elevations.

CHAPTER FIVE

CONCLUSION AND RECOMMENDATIONS

5.1. Conclusions

MASW has been used to measure shear wave velocity up to a depth of 30 m, for a major part of the GAMA. The average shear wave velocity for various depths (Vs5, Vs15, Vs30, Vs40) has been calculated and used to evaluate seismic site effect for a major part of the GAMA.

Optimal datasets were acquired via a series of tests, with various receiver-offset and spread-size parameters. Selected configurations were efficient in identifying fundamental mode of Rayleigh wave dispersion curve and minimizing the effects of incoherent noise and other signals that cause higher-mode domination at the low or high frequency end of dispersion-curve spectrum. Consequently, inversion results presented in the study, were not influenced by higher mode, thus avoiding overestimation at greater depths.

According to the National Earthquake Hazard Risk Program (NEHRP) site classes, for the top 30 m depth of soil deposits (Vs30), results of seismic site effect investigations, for residual soils of the GAMA is characterized by two (2) main site classes (C and D).

Considering residual soils derived for the GAMA geology two (2) subdivisions for site class D are suggested (D1 and D2).

Calculated mean shear wave velocity distribution with depth, suggests prevalent deep soil profiles (>30 m), especially to the south of the study area, irrespective of the topography within the area.

Areas to the south and northwest (of the study area), predominantly underlain by GAMA granitoids are classified as site class D1. Depth profiles here are especially deep, with deeply

seated bedrock (> 30 m, sometimes not encountered). These soils characterized by Vs between 180 – 360 m/s, are considered the most vulnerable, and mostly made of stiff soils with a mix of soft soils (Vs less than 180 m/s) commonly encountered at depth, suggesting soils are not uniformly compacted within depth profiles.

D2 generally covers a small part of the southeast, (lower) middle and the northeast of the study area. Seismic site response for site class D2 for the study, are also generally within Vs 180 – 360 m/s (similar in range to the D1). However, seismic site response values are derived from the residual soils of phyllite (phyllonitic) units within the GAMA.

Site class C represents the more moderate competent soils found predominantly in the (upper) central part of the study area, where residuals soils are underlain by quartz-schist and quartzite units. Soil profiles are shallower here. The depth profiles for site class C are composed of shallow soil profiles, mostly of dense soils with bedrock type velocities at depth (≈15 m, rarely seen before this depth).

In general, the observed SWV increases with depth in the area. However, the SWV from 5 m up to approximately 15 m depth is characteristically low (between 180 – 360 m/s), with several dynamic features that point to many vulnerabilities in soil competency within the first 15 m for the entire region, irrespective of topography.

5.2 Recommendations

The site classification map presented in the study, provide some preliminary information on soil conditions for the GAMA. Although it covers a major part of the GAMA it has some

limitations, and the following recommendations are suggested for future work and relevant stakeholders;

In the areas especially to the southwest of the GAMA, where seismic risk has become overwhelmingly apparent (i.e., overpopulated and poorly planned with the largest convergence of major and minor faults, historical and many recent events), distribution of shear wave velocity up to 30 m alone, is not enough to assess full damage distribution of the GAMA. At this stage, detailed soils conditions maps based on Vs30 and other geotechnical parameters correlated strongly with regional borehole studies, bedrock geometry, ground motion and other dynamic features are very urgent and important for effective seismic site safety and improved earthquake hazard assessment for the region.

MASW field measurements, with various source-receiver configurations, will further help to test constraints of the technique especially for the particular soils of the GAMA. This is important as bedrock may influence shearwave velocity distribution at shallow bedrock sites within the study area.

Many sites still remain untested and although a major part has been tested the outcome falls short of a complete regional perspective (Ga east, Accra metropolitan assembly etc not tested). The program requires comprehensive testing, covering the entire region, where results obtained will compliment work done in this study for overall regional perspective.

This suggested scale of regional Vs30 mapping calls for a substantially large financial and logistical effort by all stakeholders, at a level which cannot necessarily be accomplished as just an academic exercise.

REFERENCES

Affaton, P., Rahaman, M.A., Trompette, R. and Sougy, J. (1991). The Dahomeyide Orogen: tectonothermal evolution and relationships with the Volta basin. In: Dallmeyer, R.D., Lecorché, J.P. (Eds.). The West African Orogens and Circum-Atlantic Correlatives. Springer, New York, 95–111.

Agbossoumondé, Y., Guillot, S. and Ménot, R.P. (2004). Pan-African subduction collision event evidenced by high-P coronas in meta-norites from the Agou Massif (southern Togo). Precambrian Research, 135, 1–21

Agbossoumondé, Y., Ménot, R. P. and Guillot, S. (2001). Metamorphic evolution of neoproterozoic eclogites from south Togo (West Africa): geodynamic implications for the reconstruction of west Gondwana. Journal of African Earth Scientist, vol. 33, issue 2, 227–244.

Ahmed, S.M., Blay, P.K., Castor, S.B., Coakley, G.J., (1977). The Geology of Field Sheets No. 33 Winneba NE 59, 61 and 62. Accra. SW, NW and NE. Ghana Geological Survey, Bulletin No. 32, 1–47.

Ajibade, A.C., Wright, J., (1989). The Togo-Benin-Nigerian shield: evidence for crustal aggregation in the Pan-African belt. Tectonophysics 165, 125-129.

Aki, K. (1988). Local site effects on strong ground motion, in Proc. Earthquake Engineering and Soil Dynamics II: Recent Advances in Ground Motion Evaluation, ASCE, Park City, Utah, 27–30 June, 103–155.

Ako J. A., Wellman P. (1985). The margin of the West African craton: the Voltaian basin. Journal of the Geological Society, London 142:625–632.

Akpati, B.N., (1978). Geological structure and evolution of the Keta Basin, Ghana, West Africa. Geological Society of America Bulletin 89, 124–132

Amponsah, P.E., B.K. Banoeng-Yakubo, F. Vaccari, D. Asiedu, G. F. Panza, (2008). Seismic ground motion and hazard assessment of the Greater Accra Metropolitan Area, southeastern Ghana; The Abdus Salam Int. Centre for Theoretical Physics, Miramare-Trieste 1-19.

Anbazhagan, P., and Sitharam, T. G. (2008a). "Seismic microzonation of Bangalore." J. Earth Syst. Sci., 117(S2), 833–852.

Anbazhagan, P., and Sitharam, T. G. (2008b). "Site characterization and site response studies using shear wave velocity." J. Seismol. Earthq. Eng., 10(2), 53–67.

Anbazhagan, P., Sitharam, T.G., Vipin, K.S., (2009). Site classification and estimation of surface level seismic hazard using geophysical data and probabilistic approach. Journal of Applied Geophysics 68 (2), 219–230

Antobreh, A.A., Faleide, J.I., Tsikalas, F., Planke, S., (2009). Rift-shear architecture and tectonic development of the Ghana margin deduced from multichannel seismic reflection and potential field data. Marine and Petroleum Geology 26, 345–368.

Attoh, K. & Nude, P. M. (2008). Tectonic significance of carbonatite and ultrahigh pressure rocks in the Pan-African Dahomeyide suture zone, southeastern Ghana. Geological Society, London, Special Publications (2008); vol. 297, 217-231.

Attoh, K., Brown, L., (2008). Deep structures of the southeastern margin of the West African craton from seismic reflection data, offshore Ghana. In: Ennih, N., Liégeois, J.-P. (Eds.), The boundaries of the West African Craton, Geological Society, London, Spec. Pub., vol. 207, 499–508.

Attoh, K., Brown, L., Guo, J., Haenlein, J., (2004). Seismic stratigraphic record of transpression and uplift on the Romanche transform margin, offshore Ghana. Tectonophysics 378, 1–16.

Attoh, K., Brown, L., Haenlein, J., (2005). The role of Pan-African structures in intraplate seismicity near the termination of the Romanche fracture zone, West Africa. Journal of African Earth Sciences 43, 549–555.

Attoh, K., Dallmeyer, R.D. and Affaton, P. (1997). Chronology of nappe assembly in the Pan-African Dahomeyide orogen, West Africa: evidence from 40Ar/39Ar mineral ages. Precambrian Research, vol. 18, 153 – 171.

Ayetey, J K and Andoh, M B. (1988) Earthquake site response study of Accra area, Ghana Int. assoc. Engng. Geol. BullN38, 15–25

Bacon, M., Quaah, A.O., (1981). Earthquake activity in southern Ghana (1977–1980). Bulletin of Seismological Society of America 71 (3), 771–785.

Basile, C., Mascle, J., Guiraud, R., (2005). Phanerozoic geological evolution of then Equatorial Atlantic domain. Journal of African Earth Sciences 43, 275–282.

Black R. (Ed.), (1985). Evolution géologique de l'Afrique. Séminaire de Formation, Février 1985. Compte rendu de Conférences. CIFEG, Publication Occasionnelle 1985/4, 340.

Blarez, E., Mascle, J., (1988). Shallow structures and evolution of the Ivory Coast and Ghana's transform margin. Marine and Petroleum Geology 5, 54–64.

Blundell, D.J., (1976). Active faults in West Africa. Earth and Planetary Science Letters 31, 287–290 (Elsevier Scientific Publishing Company, Amsterdam).

Blundell, D.J., Banson, J.K.A., (1975). Interpretation of seismic reflection survey across the continental Shelf of Accra and its Bearing on Earthquakes in the Area. Report Geological Survey No. 75/1, 1–7.

Bondesen, E., Smit, A.F.J., (1972). Holocene tectonic activity in West Africa dated by archaeological methods discussion. Geological Society of America Bulletin 83 (4), 1193 1196.

Boore, D. M., W. B. Joyner, and T. E. Fumal (1997). Equations for estimating horizontal response spectra acceleration from western North American earthquakes: A summary of recent work, Seismol. Res. Lett. 68, no. 1, 29–61.

Borcherdt, R. D. (1970). Effects of local geology on ground motion near San Francisco Bay, Bull. Seismol. Soc. Am. 60, no. 1, 29–61.

Borcherdt, R.D., (1994). Estimates of site-dependent response spectra for design (methodology and justification): Earthquake Spectra, 10, 617-653.

BRRI (Building and Road Research Institute) (1990) Code for the Seismic Design of Concrete Structures. Kumasi, Ghana: Council for Scientific and Industrial Research (CSIR-INSTI)

Burke, K., (1969a.) The Akwapim Fault, a recent fault in Ghana and related faults of the Guinea Coast. Journal of Mining and Geology, Nigeria 4 (1 and 2), 29–38.

Burke, K., (1969b). Seismic areas of the guinea coast where Atlantic fracture zones reach Africa. Nature 222, 655–657.

Caby, R. (2003). Terrane assembly and geodynamic evolution of central western Hoggar: a synthesis. Journal of African Earth Scientist,Vol. 37 (3–4), 139–159.

Caby, R., Andreopoulos-Renaud, U.&Pin, C. (1989.) Late Proterozoic arc-continent and Continent-continent collision in the Pan-African trans-Saharan belt of Mali. Canadian Journal of Earth Sciences, 26, 1136–1146.

Camil J., (1984). Pétrographie, chronologie des ensembles granulitiques archéens et formations associées de la région de Man (Côte d'Ivoire): Implications pour l'histoire géologique du craton ouest africain. Thèse Doctorat d'Etat, Université d'Abidjan, 306 p.

Castaing, C., Triboulet, C., Feybesse, J.-L., Cherrement, P., (1993). Tectonometamorphic evolution of Ghana, Togo and Benin in the light of the Pan-African Brasiliano orogeny. Tectonophysics 28, 423-432.

Cramer, C. H., J. S. Gomberg, E. S. Schweig, B. A. Waldron, and K. Tucker (2004). The Memphis, Shelby County, Tennessee, seismic hazard maps, U.S. Geol. Surv. Open File Rept. 2004-1294.

Danquah, I. O. (2013). Climate change and its impacts on flooding in Accra, Greater Accra Metropolitan Assembly, 32

Deltail, J.R., Valery, P., Montadert, C., Fondeur, C., Patriat, P., Mascle, J., (1974). Continental margin in the northern part of the gulf of Guinea. In: Burk, C.,Drake, C.L. (Eds.), Geology of Continental Margins. Springer, New York, 297–311

Dobry, R., R.D. Borcherdt, C.B. Crouse, I.M. Idriss, W.B. Joyner, G.R. Martin, M.S. Power, E.E. Rinne, et al. 2000. New site coefficients and site classification system used in recent building seismic code provisions. Earthquake Spectra 16(1): 41–67.

Donohue, S., Dermot, F. & Donohue, L. A. (2013). Detection of soil compaction using seismic surface waves. Soil and Tillage Research, 128, 54-60.

Edwards, R.A., Whitmarsh, R.B., Scrutton, R.A., (1997). Synthesis of the crustal structure of the transform continental margin off Ghana, northern Gulf of Guinea. Geo-Marine Letters 17, 12 20.

EERI Housner Fellows Report (2015) Improving the Earthquake Safety of Ghana's Schools, 6 - 37

Fitches, W. R., (1970) "Pan African Orogeny in the Coastal Regions of Ghana," Nature, Vol. 226, No. 5247, 744-748.

Forbriger, T., (2003), Inversion of shallow-seismic wavefields: I. Wavefield transformation: Geophysical Journal International, 153, 719–734.

Frankel, A. D., W. J. Stephenson, and D. L. Carver (2009). Sedimentary basin effects in Seattle, Washington: Ground-motion observations and 3D simulations, Bull. Seismol. Soc. Am. 99, 1579–1611.

Green, R.A., S.M. Olson, B.R. Cox, G.J. Rix, E. Rathje, J. Bachhuber, J. French, S. Lasley, et al. 2011. Geotechnical aspects of failures at Port-au-Prince seaport during the 12 January 2010 Haiti earthquake. Earthquake Spectra 27(S1): S43–S65.

Haskell, N. A. (1953). The dispersion of surface waves on multilayered media. *Bulletin of the Seismological Society of America, 43*, 17–34.

Holzer, T.L., Padovani, A.C., Bennett, M.J., Noce, T.E., Tinsley III, J.C., (2005). Mapping NEHRP VS30 site classes: Earthquake Spectra, 21, 161-177.

https://www.weforum.org/agenda/2019/05/ghana-is-set-to-be-the-worlds-fastest-growing economy-this-year-according-to-the-imf/, accessed 01/05/2021, 17:00GMT

IBC. 2000. International Building Code-2000, 5th Edition. International Code Council: Inc., Falls Church, VA.

ICC (International Code Council). 2000. 2000 international building code. Washington, DC: ICC.

ICC (International Code Council). 2006. 2006 international building code. Washington, DC: ICC.

International Code Council (ICC), (2000), International Building Code 2000.

International Code Council (ICC), 2006, International Building Code 2006.

Ivanov, J., Miller, R.D., Lacombe, P., Johnson, C.D., and Lane, J.W. Jr., (2006). Delineating a shallow fault zone and dipping bedrock strata using multichannel analysis of surface waves with a land streamer: Geophysics, 71(5), A39–A42.

Junner, N.R., (1941). The Accra Earthquake of 22nd June, 1939. Gold Coast Geological Survey, Bull. 13, 3–41, with 4 Plates, second printing. Ghana Publishing Corporation, Assembly Press, Accra, Ghana, (1985) (In the same Bulletin, the following papers are published: Tillotson, E.: Notes on the Accra Earthquake of 22nd June, 1939, 42–59. Deakin, C.S.: Engineering Aspects of the Accra, Earthquake. 60–70).

Kanli, A.I., Tildy, P., Pronay, Z., Pinar, A., Hemann, L. (2006), Vs_{30} mapping and soil classification for seismic site effect evaluation in Dinar region. SW Turkey, Geophysical Journal International 165, 223–235.

Kesse G.O. (1985). The Mineral and Rock Resources of Ghana; A. A. Balkema Publishers, the Netherlands - Rotterdam, Boston.

Kim, D.S., C.K. Chung, C.G. Sun, and E.S. Bang. 2002. Site assessment and evaluation of spatial earthquake ground motion of Kyeongju. Soil Dynamics and Earthquake Engineering 22(5).

Kausel, E. & Roësset, J. M. (1981). Stiffness matrices for layered soils. *Bulletin of the Seismological Society of America, 71*(6), 1743-1761.

Lee, S.H., C.G. Sun, J.K. Yoon, and D.S. Kim. 2012. Development and verification of a new site classification system and site coefficients for regions of shallow bedrock in Korea. Journal of Earthquake Engineering 16(6): 795–819.

Lin, C.-P., Chang, C.-C. & Chang, T.-S. (2004), The Use of MASW Method in the Assessment of Soil Liquefaction Potential. *Soil Dynamics and Earthquake Engineering*, *24*, 689-698.

Louie, J. N., (2001), Faster, better: Shear-wave velocity to 100 meters depth from refraction microtremor arrays: Bulletin of the Seismological Society of America, 91, no. 2, 347–364.

Multichannel Analyses of Surface Waves (MASW). (n.d.d). Inversion Analysis of Surface Waves. Retrieved May 10, 2021 from http://www.masw.com/InversionAnalysis.html

Mascle, J., Blarez, E., (1987). Ivory Coast-Ghana Margin: Model of a Transform Margin: Abstract. AAPG Bulletin, 71.

Mascle, J., Sibuet, J.C., (1974). New pole for early opening of South Atlantic. Nature 252, 464 465.

McCallien, W.J., (1962). The rocks of Accra. A guide to the coast along High street. 1- 74

McMechan, G. & Yedlin, M. J. (1981). Analysis of dispersive waves by wave field trans-formation. *Geophysics, 46*(6), 869-874.

Miller, R.D., Xia, J., Park, C.B., and Ivanov, J., (1999). Multichannel analysis of surface waves to map bedrock: in The Leading Edge, 18 (12), 1392–1396.

Ministry of Local Government. (MGL 1992). Strategic Plan for the Greater Accra Metropolitan Area. Volume 1: Context Report. Accra: Department of Town and Country Planning, Ministry of Local Government.

Montalvo-Arrieta, J.C., Sánchez-Sesma, F.J., Reinoso, E., (2002). A virtual reference site for the Valley of Mexico: Bulletin of the Seismological Society of America, 92, 1847-1854.

Muff, R., Efa, E., (2006). Environmental and Engineering Geology for urban planning in the Accra-Tema area, Geological Service Department- Ghana and federal institute for Geoscience and natural resources, Hannover, Germany.

Nazarian, S., Stokoe Ii, K.H., Hudson, W.R., (1983). Use of spectral analysis of surface waves method for determination of moduli and thicknesses of pavement systems, Transportation Research Record 930, 38–45.

Ne´de´lec, A., Affaton, P., France-Lanord, C.,Charrie` Re, A. & Alvaro, J. (2007.) Sedimentology and chemostratigraphy of the Bwipe Neoproterozoic cap dolostones (Ghana, Volta Basin): a record of microbial activity in a peritidal environment. Comptes Rendus Geosciences, 339, 223–239 and erratum Comptes Rendus Geosciences, 339, 516–518.

NEHRP (2003). "Recommended provisions for seismic regulations for new buildings and other structures," FEMA 450 . Building Seismic Safety Council, National Institute of Building Sciences, Washington, DC.

NEHRP (2009). "Recommended provisions for seismic regulations for new buildings and other structures," FEMA 750. Building Seismic Safety Council, National Institute of Building Sciences, Washington, DC.

Orozco, M. C. (2003). Inversion Method for Spectral Analysis of Surface Waves (SASW). (Doctoral dissertation, Georgia Institute of Technology, Atlanta, GA). Retrieved from https://smartech.gatech.edu/bitstream/handle/1853/5124/OROZCO_MARIA _C_200405_phd.pdf

Park, C. B., Miller, R. D. & Xia, J. (1997). Summary report on surface-wave project at Kansas Geological Survey (KGS). [Open-file Report]. Lawrence, KS: Kansas Geological Survey.

Park, C. B. and Carnevale, M. (2010). Optimum MASW Survey -Revisit after a Decade of Use. In Fratta, D. O., Puppala, A. J. & Muhunthan, B (editors), *GeoFlorida 2010: Advences in Analysis, Modeling and Design* (pp. 1303-1312). doi: 10.1061/41095(365)130

Park, C. B., Miller, R. D., and Xia, J. (1999) Multichannel analysis of surface waves, Geophysics, 64, 800–808.

Park, C.B., Miller, R.D., Xia, J., and Ivanov, J., (2007) Multichannel analysis of surface waves (MASW), active and passive methods: in The Leading Edge, 26 (1), 60–64.

Park, S., Elrick, S., (1998). Predictions of shear-wave velocities in southern California using surface geology: Bulletin of the Seismological Society of America, 88, 677-685

Park, C. B. & Shawver, J. B. (2009). Multi-source offset MASW survey. *Proceedings of the Symposium on the Application of Geophysics to Engineering and Environmental Problems (SAGEEP 2009), Fort Worth, Texas, March 29-April 2*.

Pescina, J. U. (2013). The Economic Base of Accra, Ghana, Advanced Issues in Development Planning, 2

Pichon, X. L and D. E. Hayes, (1971) "Marginal Offsets, Fractures Zones, and the Early Opening of the South Atlantic. Journal of Geophysical Research, Vol. 76, No. 26, 6283-6293

Quaah, A. O., (2013). Ghana News Agency, Earthquake: Why Nuclear Power Stations are not Suitable for Ghana, GhanaWeb, available online: http://www.ghanaweb.com/GhanaHomePage/features/artikel.php?ID=282868, 20 August 2013, accessed 1 May 2015.

Quaah, A.O., (1980). Microseismicity, past seismic activity and seismic risk in southern Ghana. Ph.D. Thesis. University of London. 23-198.

Quaah, A.O., (1982.) A study of past earthquakes in southern Ghana using intensity data. Tectonophysics 88, 175–188.

Richart, F.E., Hall, J.R., and Woods, R.D., (1970). Vibrations of soils and foundations: Prentice-Hall, Inc., 414

Robertson, P.K. and Wride, C.E. (1998). "Evaluating cyclic liquefaction potential using the cone penetration test."Canadian Geotech. J., 35(3), 442-459

Rodríguez-Marek, A., Bray, J.D., Abrahamson, N.A., (2001) An empirical geotechnical seismic site response procedure: Earthquake Spectra, 17, 65-87.

Ryden, N., C. B. Park, P. Ulriksen, and R. D. Miller, (2004), Multimodal approach to seismic pavement testing: Journal of Geotechnical and Geoenvironmental Engineering, 130, 636–645

Ryden, N. & Park, C. B. (2006) Fast Simulated Annealing Inversion of Surface Waves on Pavements using Phase Velocity Spectra. *Geophysics*, *71*(4), R49-R58.

Socco, L. V., D. Boiero, S. Foti, and R. Wisén, (2009), Laterally constrained inversion of ground roll from seismic reflection records: Geophysics, 74, no. 6, G35–G45.

Socco, L. V. & Boiero, D. (2008). Improved Monte Carlo inversion of surface wave data. *Geophysical Prospecting*, *56*(3), 1365-2478.

Socco, L. V., D. Boiero, S. Foti, and R. Wisén, (2009), Laterally constrained inversion of ground roll from seismic reflection records: Geophysics, 74, no. 6, G35–G45.

Stewart, J.P., Liu, A.H., Choi, Y., (2003) Amplification factors for spectral acceleration in tectonically active regions: Bulletin of the Seismological Society of America, 93, 332-352.

Sun, C.G., C.K. Chung, and D.S. Kim. 2005. A proposition of site coefficients and site classification system for design ground motions at inland of the Korean Peninsula. Journal of the Korean Geotechnical Society 21(6): 101–115 (in Korean).

Sutherland, A. J., and Logan, T. C., (1998), SASW measurement for the calculation of site amplification Earthquake Commission Research Project 97/276: unpub. Central Laboratories Report 98522422, Lower Hutt, New Zealand, 22

Schwab, F. A. & Knopoff, L. (1970). Surface-wave dispersion computations. *Bulletin of the Seismological Society of America*, *60*, 321-344.

Sykes, R.L., (1978). Intraplate Seismicity, Reactivation of Pre-existing Zones of Weakness, Alkaline magmatism and other Tectonism Postdating Continental Fragmentation. Reviews of Geophysics and space Physics, 16, No.4, 621 - 682.

Tevendale, W.B., (1957). Geology of the Volta River Project, Ghana Geological Survey Bulletin, vol. 20, 119

Tokeshi, K., Leo, C. J., and Liyanapahirana, S. (2013) Comparison of ground models estimated from surface wave inversion using synthetic microtremors, Soil Dyn. Earthq. Eng., 49, 19–26

Tokimatsu, K., Kuwayama, S., Tamura, S. & Miyadera, Y. (1991). Effects of Multiple Modes on Rayleigh Wave Dispersion Characteristics. *Soils and Foundations, 31*(2), 153 163.

Thomson, W. T. (1950). Transmission of elastic waves through a stratified solid medium. *Journal of Applied Physics, 21,* 89–93.

Trompette, R. (1997). Neoproterozoic (600 Ma) aggregation of Western Gondwana: a tentative scenario. Precambrian Research, vol. 82, 101–112.

Vilanova, S.P., Fonseca, J., and Oliveira, C.S. (2012). Ground-Motion Models for Seismic-Hazard Assessment in Western Iberia: Constraints from Instrumental Data and Intensity Observations. Bulletin of the Seismological Society of America, 102:1, 169-184.

Wald, D.J., and T.I. Allen. 2007. Topographic slope as a proxy for seismic site conditions and amplification. Bulletin of the Seismological Society of America 97(5): 1379–1395.

Wills, C.J., M. Petersen, W.A. Bryant, M. Reichle, G.J. Saucedo, S. Tan, G. Taylor, and J. Treiman. 2000. A site-conditions map for California based on geology and shear-wave velocity. Bulletin of the Seismological Society of America 90(6B): 187–208.

Wills, C.J., M. Petersen, W.A. Bryant, M. Reichle, G.J. Saucedo, S. Tan, G. Taylor, and J. Treiman. 2000. A site-conditions map for California based on geology and shear-wave velocity. Bulletin of the Seismological Society of America 90(6B): 187–208.

Xia, J. R. D., Miller, and C. B. Park., (1999) Estimation of near-surface velocity by inversion of Rayleigh waves: Geophysics, 64, 691–700.

Xia, J., R. D. Miller, and C. B. Park, (1999), Estimation of near-surface velocity by inversion of Rayleigh waves: Geophysics, 64, 691–700.

Xia, J., R. D. Miller, C. B. Park, and G. Tian, (2003), Inversion of high frequency surface waves with fundamental and higher modes: Journal of Applied Geophysics, 52, 45–57.

Xu, Y., J. Xia, and R. D. Miller, 2006, Quantitative estimation of minimum offset for multichannel surface-wave survey with actively exciting source: Journal of Applied Geophysics, 59, 117–125, doi:10.1016/j.jappgeo.2005.08.002.

Yacé I., (1984). Le Précambrien de l'Afrique de l'Ouest et ses correlations avec le Brésil oriental. Rap. Final Projet PICG.

Youd, T.L., Idriss, I.M., Andrus, R.D., Arango, I., Castro, G., Christian, J.T., Dory, R., Finn, W.D.L., Harder, L.F., Hynes, M.E., Ishihara, K., Koester, J.P., Liao, S.S.C., Marcuson, W.F., Martin, G.R., Mitchell, J.K., Moriwaki, Y., Power, M.S., Robertson, P.K., Seed, R.B., and Stokoe, K.H. (2001)."Liquefaction Resistance of Soils: Summary Report from 1996

Zeng, C., Xia, J., Miller, R. D., Tsoflias, G. P. & Wang, Z. (2012). Numerical investigation of MASW applications in presence of surface topography. Journal of Applied Geophysics, 84, 52-60.